Arabian Journal for Science and Engineering (2020) 45:5803–5831
https://doi.org/10.1007/s13369-020-04587-3

RESEARCH ARTICLE-MECHANICAL ENGINEERING

A Multi-response Optimal Design of Bridge Amplification Mechanism Based on Efficient Approach of Desirability, Fuzzy Logic, ANFIS and LAPO Algorithm

Ngoc Le Chau[1] · Ngoc Thoai Tran[1] · Thanh-Phong Dao[2,3]

Received: 18 December 2019 / Accepted: 26 April 2020 / Published online: 6 May 2020

Abstract
Compliant mechanism is becoming increasingly to be a part of precision engineering, robotics, and bioengineering thanks to excellent advantages of free friction, free lubricant, no backlash, monolithic structure, and minimal assembly. However, design and analysis of compliant mechanism has been facing challenges due to a coupling of kinematic and mechanical behaviors in comparison with rigid-body counterparts. Particularly, considering a multi-response optimization design, the problem is becoming more and more complex. Thus, this article proposes a new efficient hybrid methodology to resolve multi-objective optimization design of compliant mechanisms. A bridge amplification mechanism with three numerical examples is a case study to demonstrate the effectiveness of the proposed optimizing technique. A hybridization is developed by combining finite element method, statistical method, desirability function approach, fuzzy logic system, adaptive neuro-fuzzy inference system (ANFIS), and lightning attachment procedure optimization (LAPO). A 3D finite element model for the bridge amplification mechanism is designed, and then Box–Behnken design is employed to construct numerical experiments. The sensitivity of geometrical parameters of the mechanism is investigated through analysis of variance and Taguchi approach to make a few populations for the LAPO. Subsequently, desirability values of the displacement and safety factor of the mechanism are determined, and the results are transferred into the fuzzy logic system. The output of this system is considered as single combined objective function. By developing the ANFIS structure, the refined design variables are well mapped with the output of FIS. Finally, LAPO algorithm is adopted for solving the multi-objective optimization problem for the mechanism. The results reveal that the proposed method is more efficient than the Taguchi-based fuzzy logic. Besides, the performances of the proposed method are superior to the Jaya algorithm and TLBO algorithm through Wilcoxon signed rank test and Friedman test. The results of this article can be useful for complex optimization problems.

Keywords Compliant mechanism · Bridge amplification mechanism · Desirability · Fuzzy logic system · Adaptive neuro-fuzzy inference system · Multi-objective optimization · Lightning attachment procedure optimization · Statistical analysis

1 Introduction

Bridge amplification mechanism (BAM) is an important part of compliant mechanisms in highly precise engineering. The motions of the BAM are based on storing the elastic energy of flexure hinges [1–3]. It benefits of a monolithic structure, lightweight, and free friction without bearings or kinematic-based joints [4–6]. In the field of compliant mechanisms [7], it is well known that the important performances include a large displacement, a minimal stress, a high frequency, a high safety factor, and a small parasitic error. Considering a real application of the BAM, the displacement, safety factor, and stress are considered as the three most significant

✉ Thanh-Phong Dao
daothanhphong@tdtu.edu.vn

[1] Faculty of Mechanical Engineering, Industrial University of Ho Chi Minh City, Ho Chi Minh City, Vietnam

[2] Division of Computational Mechatronics, Institute for Computational Science, Ton Duc Thang University, Ho Chi Minh City, Vietnam

[3] Faculty of Electrical and Electronics Engineering, Ton Duc Thang University, Ho Chi Minh City, Vietnam

characteristics. Compliant mechanism is becoming promisingly to alternate for rigid-body mechanisms in precision engineering and robots, microelectromechanical systems (MEMs), bioengineering, and so forth. However, modeling and analyzing the above-mentioned performances are facing difficulties. When conducting a multiple-performance optimization problem for compliant mechanisms, it is more and more complicated.

During the last decades, there have been more efforts to conduct the design, analysis, and synthesis for compliant mechanisms, e.g., kinematic-based methods [8–11]. Besides, a lot of techniques have been developed, such as pseudo-rigid-body model (PRBM) [12, 13], Castigliano's second theorem [14], compliance matrix method [15], elastic beam theory [16], two-port dynamic stiffness model [17], empirical method [18], beam constraint model [19], Euler–Bernoulli beam theory [20], and finite element method [21]. The PRBM is limited in estimating highly nonlinear deformation of flexure hinges because the characteristic parameters of the PRBM are strongly dependent on the number of torsional springs and location of these springs. In addition, under complex loads and complicated structures, PRBM is not still suitable. So, the approximations of the PRBM are significant for simple architectures. Castigliano's second theorem can predict the strain energies of flexure hinges, e.g., tensile, shear, and bending strains, but is also limited for complex structures. Compliance matrix method is becoming more difficult when compliant mechanisms subject multiple actuation forces. Elastic beam theory is similar to Castigliano's second theorem and it still difficult for modeling. Based on two-port dynamic stiffness model, the performances of compliant mechanisms can be resolved, but it is a challenge for irregular structures. Empirical modeling can estimate the performances with a high accuracy, but it is time-consuming. Beam constraint model cannot precisely predict a large deformation of flexure hinges. Meanwhile, finite element method (FEM) has higher prediction accuracy over analytical approaches because it discretizes compliant mechanisms into elements and nodes. Although the mentioned analytical methods are still valuable in advancing of compliant mechanisms, the uses of them are facing challenges for more complex compliant mechanisms, e.g., irregular shapes of flexure hinges, multi-axis flexure hinges, and a large deflection. In the other word, the estimating accuracy of modeling is still challenging due to a coupling of kinematic and mechanical behaviors of compliant mechanisms. When optimizing multiple performances of the BAM simultaneously, it becomes a complex problem. Hence, FEM is chosen as an effective tool to analyze the highly nonlinear deformation of the BAM. Up to now, there have been three types of optimization for compliant mechanisms, including topology optimization [22], shape optimization, and size optimization [20, 23, 24]. Among these types, the size optimization is critical important to improve the performances. According to the field of compliant mechanism [25], the displacement is always conflicted with the safety factor. From reviewing the literature review, the motivation of this article is to develop a computational intelligence approach to solve the multi-objective optimization (MOO) problem for the BAM. The purpose of MOO problem is to reach a trade-off between the displacement and safety factor. Nowadays, MOO problem has received a great interest in the field of compliant mechanisms [26–28].

The results of previous studies in the literature review indicated that physical performances of the BAM are very sensitive to a change in shape, material, or geometrical parameters. Shape and material are directly chosen according to customer's requirements. Meanwhile, geometrical parameters have strongly affected the performances. Therefore, the most significant parameters and the nonsignificant parameters should be identified. The most key parameters, considered as design variables, always contribute on the physical outcomes of the BAM. Meanwhile, the less contributing parameters should be suppressed during the MOO problem because they cause a high computational cost. So, searching such geometrical parameters is the first motivation of this article.

Considering the modeling process of fitness functions for the BAM, a mathematical model is established through analytical approaches such as pseudo-rigid-body model [29], semi-analytical model [30], and compliance matrix [31] before dealing with a MOO problem. But the analytical methods are limited to feature the performances of compliant mechanisms, especially for the BAM. When using the formed equations, the later optimal solutions may be imprecise since the modeling is an uncompleted approximation. In order to overcome this limitation, data-driven approach is an advantageous tool to deal with the MOO problem. Data-driven approach is called as a surrogate-based method which directly maps inputs and outputs. Several common approaches can be utilized for MOO problem, e.g., desirability function approach (DFA) [32], gray relational analysis (GRA) [33], and Taguchi method-based fuzzy logic (TMFL) [34]. However, both the DFA and GRA require a weight factor for each objective function, but weighting is largely dependent on experience or users. Meanwhile, the TMFL does not require any weight factor, but it searches optimal results, considered as local solutions, because the Taguchi method finds discrete solutions. In order to avoid a local result, surrogate models are employed, such as response surface method [35], kriging technique [36], artificial neural network [37–39], and adaptive neuro-fuzzy inference system (ANFIS) [40–42]. Among them, the ANFIS is more effective technique to formulate a virtual fitness function. Therefore, the ANFIS is chosen to model process of the fitness function for the BAM.

It is noted that nature-based metaheuristic algorithms have been developing increasingly, e.g., genetic algorithm [43], particle swarm optimization [44], differential evolution [45], cuckoo search algorithm [46], and other algorithms [47–50]. More recently, several algorithms with less or non-tuned parameters have been developed such as teaching learning-based algorithm (TLBO) [51, 52], Jaya algorithm [53], and lightning attachment procedure optimization (LAPO) algorithm [54]. Among three less-parameter algorithms, LAPO algorithm is an effective tool for a lot of engineering areas, but it has not been applied for the bridge mechanism yet. Therefore, this article chooses LAPO algorithm to extend to MOO design for the bridge mechanism.

Summarily, new contributions of this study are covered as follows: (i) The performances of the BAM are effectively analyzed via using the nonlinear FEM. (ii) The less influencing parameters and the most significant parameters are identified. And then, the nonsignificant parameters are refined to redetermine a few new populations for LAPO algorithm. This process helps to decrease the complexity of optimization problem. (iii) The desirability values of two performances of the BAM are calculated and transferred into the fuzzy inference reasoning (FIS) system to generate a single combined objective function. (iv) The ANFIS structure is developed to combine the refined design variables and the output of FIS. (v) LAPO algorithm is extended for solving the MOO problem of the BAM. (vi) The proposed optimizing scheme provides a computational intelligence approach by integrating statistical methods, FEM, fuzzy logic system, ANFIS, and metaheuristic algorithms, which can be extended for other optimization problems.

The goal of this paper is to develop a new hybrid optimizing method for solving the MOO problem of compliant mechanisms. The BAM is a case study to illustrate the performance efficiency of the proposed method. Three numerical examples of the BAM are studied. The remaining structure of this article is summarized as follows. The proposed hybrid method is presented in Sect. 2. Section 3 demonstrates the structural design and simulation formulation for the BAM. Results and discussion are presented in Sect. 4. The analysis of case studies is given in Sect. 5. A comparison of the proposed method with Jaya algorithm and TLBO algorithm is discussed in Sect. 6 by using the Wilcoxon signed rank test and Friedman test. Conclusions and future work are presented in Sect. 7.

2 Proposed Hybrid Methodology

Figure 1 describes the proposed hybrid methodology. The proposed method is utilized for solving MOO design problem for the BAM. Practically, the performances of the mechanism require a large displacement and a high safety factor. In order to achieve an improvement in desired objectives, the performances of mechanism are optimized simultaneously. The proposed hybrid methodology consists of five key phases: (i) mechanical design and analysis, (ii) desirability calculation, (iii) fuzzy logic system, (iv) ANFIS modeling, and (v) MOO problem by LAPO algorithm. Each phase includes sub-steps.

Phase 1: Design and analysis

Initially, analysis phase defines a mechanical design problem. In this study, the BAM is numerically investigated to validate the performance effectiveness of proposed methodology. This phase experiences the following main steps.

Step 1 Architecture design

As mentioned discuss, the BAM needs a large displacement but must guarantee a high safety factor. In addition, equivalent stress must be lower than the yield strength of proposed material to avoid plastic failures.

Step 2 Predetermine geometrical parameters

A mechanical structure has a lot of geometrical parameters affecting the displacement, the safety factor, and the stress. Influences of the geometrical parameters are evaluated through a sensitivity investigation later.

Step 3 Define output performances

After determining the initial design variables, a large displacement and a high safety factor are assigned as two desired outputs. In order to satisfy a working strength, a minimal stress is a critical constraint.

Step 4 Create 3D finite element model

This step initializes a 3D FEM model, and then, finite element analysis (FEA) is implemented to retrieve the numerical data.

Step 5 Box–Behnken design

After creating the 3D model, an experimental matrix is initialized by using Box–Behnken design (BBD).

Step 6 Collect numerical data

Boundary conditions, load, and material are set up for the 3D model. Subsequently, a set of numerical data is collected through simulations.

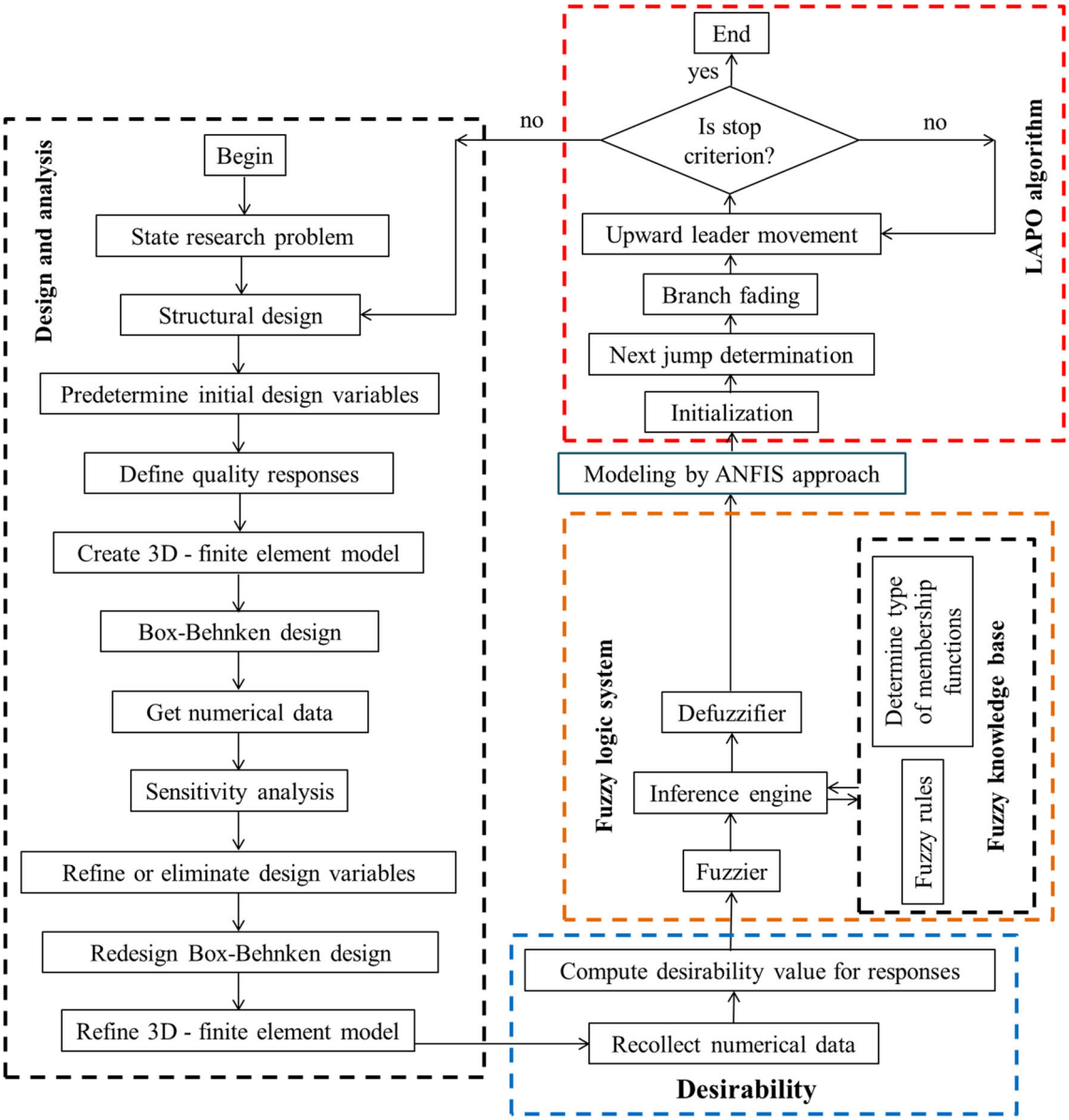

Fig. 1 Flowchart of proposed hybrid approach

Step 7 Sensitivity analysis

Sensitivity investigation is an important step to determine the most significant parameters, named as design variables, and the nonsignificant parameters are neglected during the further optimization process. This process is conducted through analysis of variance (ANOVA) and the Taguchi method.

Step 8 Refine and eliminate design variables

Based on the results of sensitivity analysis in step 7, the results of refining parameters create several new populations for the LAPO later. This is a preparing step for further optimization process. The goal of step 8 is to determine a suitable searching space so as to reduce the computational cost.

Step 9 Redesign Box–Behnken design

There will be several new spaces of design variables are created in step 8, and step 9 will rebuild the 3D model. Then, the numerical experiments are set up by using BBD again.

Step 10 Refine finite element model

After new experimental matrix is initialized, the key design variables are redetermined for 3D FEM model. Subsequently, simulations are implemented to get the numerical data for each case study.

Phase 2: Desirability calculation

Step 11 Recollect numerical data

Based on experimental matrix in step 9 and 3D FEM model in step 10, numerical data for each of case studies are collected through FEA simulations.

Step 12 Compute desirability value for performances

Based on desirability function approach [55], the exponential type is transformed to each response into a desirability function. Principle of this technique is to compute *i*th quality response (y^*) to become *i*th desirability (d_i), and then, all values of desirability are combined into a single desirability function (D). Desirability value can reach unity when the response's target is achieved, and otherwise. Each individual desirability function is divided into three types based on user's specific demand. It includes three target types, i.e., smaller-the-best, higher-the-best, and normal-the-best. Desirability for two specifications of the mechanism is computed. Displacement is millimeter, while safety factor has no unit. Based on calculating the desirability, a such influence of unit is neglected. Hence, such difference no longer affects a later optimal solution.

Smaller-the-best The response's value is expected lower than an upper limit. The desirability function is identified by

$$\begin{aligned} d_i &= 0, \quad y^* \geq U_b \\ d_i &= \left(\frac{y^* - U_b}{L_b - U_b}\right)^r, \quad L_b \leq y^* \leq U_b \\ d_i &= 1, \quad y^* \leq L_B, \end{aligned} \tag{1}$$

where d_i is the desirability value. y^* is *i*th response, and L_b and U_b are lower and upper limits of the response, respectively.

Normal-the-best The response's value is expected toward a target value (T). The desirability function can be determined by

$$\begin{aligned} d_i &= \left(\frac{y^* - L_b}{T - L_b}\right)^p, \quad L_b \leq y^* \leq T \\ d_i &= \left(\frac{y^* - U_b}{T - U_b}\right)^q, \quad T \leq y^* \leq U_b \\ d_i &= 0, \quad y^* \leq L_b \quad \text{or} \quad y^* \geq U_b \\ d_i &= 1, \quad y^* = T \end{aligned} \tag{2}$$

where p and q are specific parameters defined by users (p, $q>0$) which determine shape of d_i.

Higher-the-best The response's value is expected higher than a lower limit. The desirability function can be described by

$$\begin{aligned} d_i &= 0, \quad y^* \leq L_b \\ d_i &= \left(\frac{y^* - L_b}{U_b - L_b}\right)^r, \quad L_b \leq y^* \leq U_b \\ d_i &= 1, \quad y^* \geq U_b, \end{aligned} \tag{3}$$

where r is the desirability function index.

All individual desirability's values of the displacement and safety factor are transformed into overall desirability, D, which is considered as a single quality index. This index is determined by assigning corresponding weight factor for different quality responses. However, weight factor of each response is dependent on priority or customer's demands. A combined desirability index is computed as

$$D = \left((d_1)^{w_1}(d_2)^{w_2}\cdots(d_n)^{w_n}\right)^{\frac{1}{\sum w_i}} \tag{4}$$

where D is the overall desirability index and w_i is weight of ith response. D is equal to one as each d_i is also equal to one. Otherwise, at least one of d_is is zero and D is zero.

In the present work, a larger type is used for both the displacement and safety factor. In the past, in order to solve a MOO problem, a set of optimal parameters may be found by maximizing the single quality index D. Although this approach is still an effective tool, an optimal result is varied when the weight factor of each response is changed. It may result an imprecisely optimal value. In order to overcome this uncertainty, a fuzzy logic system is then developed to deal with all individual values of desirability of both responses since this system does not require any weight factor.

Phase 3: Fuzzy logic reasoning system

A fuzzy logic reasoning system includes knowledge base, fuzzifier, inference engine, and defuzzifier. Details can be briefly described as follows [56]: (i) Fuzzifier plays a role to transform real value into a fuzzy system. Inputs of the fuzzy logic system are called as crisp values which contain precise information of a real world. Through the fuzzifier, real value is transformed into linguistic variable. (ii) Knowledge base consists of rule base that forms a number of fuzzy rules (if–then). Moreover, the knowledge based contains a database which defines membership function (MF) of the fuzzy sets. (iii) Inference engine system of the FIS is considered as decision making based on fuzzy rules. It handles how the rules are combined. (iv) Defuzzifier transfers the output of the FIS into a crisp value. In the defuzzification method, centroid method is used to the transformation. The output of FIS, a non-fuzzy value, is called as a multi-characteristic performance index (MPCI).

In order to implement the FIS, Mamdani method is employed in the present paper. Subsequently, trapezoidal MFs are adopted for the inputs and outputs of the FIS so

as to form fuzzy sets. MFs are in the range from zero to one, and MFs can describe the way a variable matches a fuzzy set. Inputs and outputs of fuzzification system are then transformed into linguistic variables. The trapezoidal MFs are defined as

$$\mu_A(x,k,l,m,p) = \begin{cases} \frac{(x-k)}{(l-k)} & k \le x \le l \\ 1 & l < x < p \\ \frac{(x-m)}{(p-m)} & p \le x \le m \\ 0 & x \le k \quad \text{or} \quad m \le x \end{cases}, \tag{5}$$

where μ_A notes the MFs, while k, l, m, p are the x coordinates of the membership function.

In this study, desirability values of displacement and safety factor are calculated, and then, they are considered as two input variables for the FIS. These linguistic input variables will be combined into an output for the FIS. The trapezoidal MFs are employed for both the fuzzification and defuzzification. The following fuzzy rules are briefly described.

Fuzzy rule: if x_{1i} is A_1 and x_{2i} is B_{1i} then y_i is C_i
else $(i = 1, 2, 3, \ldots, n)$

where x_{1i} and x_{2i} are the two ith inputs and yi is the ith output. A_i, B_i, and C_i are defined by corresponding MFs (μ_{Ai}, μ_{Bi}, and μ_{Ci}), and these parameters are regarded as fuzzy subsets.

In order to compute the fuzzy logic reasoning, max–min operation of Mamdani is adopted. Subsequently, the FIS output is retrieved. The MFs of the FIS output can be described by

$$\mu_{ci}(y_i) = \max\left[\min_j\left\{\mu_{A_{1i}}(x_1), \mu_{A_{2i}}(x_2), \ldots, \mu_{A_{si}}(x_s)\right\}\right], \quad i = 1, 2, \ldots, n. \tag{6}$$

At last, the FIS output is transformed into real value through the defuzzification. Subsequently, a non-fuzzy value y_0, which is called as MPCI, is defined by

$$y_0 = \frac{\sum y_i \mu_{C0i}(y_i)}{\sum \mu_{C0i}(y_i)}. \tag{7}$$

Based on the theory of FIS, the best solution for overall responses and a set of optimal design variables can be found by maximizing the MPCI index through Taguchi method. This technique is divided into three types as: (i) higher-the-better, (ii) normal-the-best, and (iii) smaller-the-better. The larger-the-better type is chosen for maximizing the MPCI, which is described as

$$\eta = -10\log\left(\frac{1}{n}\sum_{i=1}^{n}\frac{1}{\text{MPCI}_i^2}\right), \tag{8}$$

where $MPCI_i$ is ith MPCI index of the FIS and n the number of ith experiment's repetition.

According to the TMFL [34], some optimal candidates may be local optimum solutions. The reason is because the Taguchi technique is employed to minimize or maximize a single fitness function in terms of discrete values. Meanwhile, a real problem desires to search a global optimum solution. In order to overcome this situation, ANFIS is then extended to model the MPCI, and the MOO design for the BAM can be effectively solved by using LAPO algorithm.

Phase 4: Adaptive neuro-fuzzy inference system

As aforementioned, the FIS is a modeling technique in terms of linguistic variables where Mamdani method is used for the FIS. Meanwhile, ANFIS is an artificial technique which is developed by integrating neural network and the FIS. Nowadays, ANFIS is considered as an intelligent modeling which creates a connection between inputs and outputs. In theory of ANFIS, the Sugeno model is employed to create fuzzy rules [57]. The fuzzy rules for ANFIS model can be defined as

$$\text{if } x_1 \text{ is } A_1 \text{ and } x_2 \text{ is } A_2, \text{ then } y = a \times x_1 + b \times x_2 + c \tag{9}$$

where x_1 and x_2 are the inputs with respect to A_1 and A_2 are the fuzzy sets, y is the output, and a, b, c are the constant values.

Figure 2 illustrates ANFIS structure which consists of five-layer feed-forward neural network.

Layer 1 is the fuzzification layer that assigns the membership degrees for input factors based on the given MFs. The output of layer 1 can be described as

$$M_1^i = \mu A_i(x) \tag{10}$$

where x is the input with respect to node ith, A_i is a linguistic label, and M_1^i is the MFs of A_i.

Layer 2 includes the fuzzy rule and a rule node which gets inputs and identifies firing strength of the rule. Each node is labeled as a circle node, Π. Each node output can be defined as.

$$w_i = \mu A_i(x) \times \mu A_i(y) \ldots i = 1,\ 2,\ 3,\ \ldots,\ n. \tag{11}$$

Layer 3 is a normalized layer which is used to estimate a ratio of firing strength of a given rule to total of firing strengths of all rules. Every node is labeled a circle node, N. In this layer, $\bar{w}$ is named for normalized firing strength of rules and defined as:

$$\bar{w} = \frac{w_i}{w_1 + w_2 + w_3, \ldots, +w_n}, \quad i = 1, 2, 3, \ldots, n. \tag{12}$$

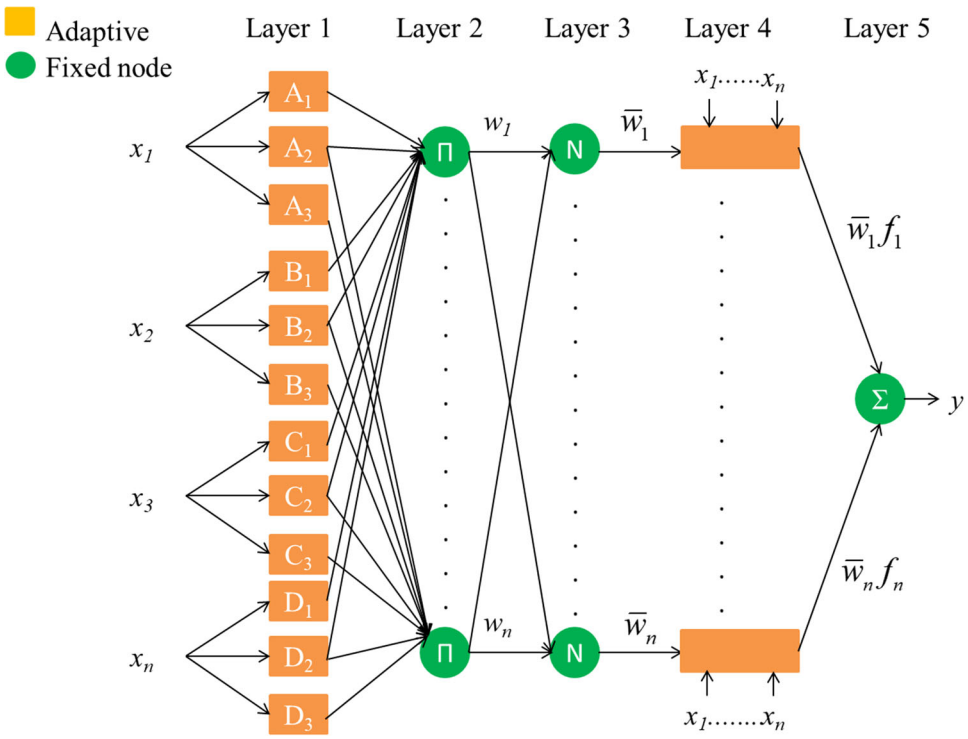

Fig. 2 The ANFIS

Layer 4 is defuzzification process and ith node is a labeled as square node by

$$M_1^i = \bar{w}_i f_i = \bar{w}_i (ax + by, \ldots, c), \quad i = 1, 2, 3, \ldots, n. \tag{13}$$

Layer 5 is an overall output, sum of all signals, which is defined as:

$$M_5^i = \sum_i \bar{w}_i f_i \frac{\sum_i w_i f_i}{w_i}. \tag{14}$$

In this article, the trapezoidal MFs are adopted for the ANFIS as well.

Phase 5: Lightning attachment procedure optimization algorithm

LAPO is a new algorithm based on physically lightning phenomena [54, 58, 59]. The LAPO benefits of a free parameter tuning. Hence, this algorithm can efficiently solve a lot of different engineering problems, e.g., gear train design, pressure vessel designs, beam, cantilever beam design, and welding, and the results demonstrated that LAPO is superior to other metaheuristic algorithms [54, 58, 59]. From the excellent advantages of the LAPO algorithm, this study chooses the LAPO algorithm to expand it to the field of compliant mechanism. It consists of five main phases as follows.

Step 1 Initialization

Unlike previous studies, the present work generates a few new search spaces based on the sensitivity results in previous steps. The LAPO also needs an initial population, N_p, within a search space of design variables. Each individual in N_P is a vector comprising n design variables $\mathbf{X} = (x_1, x_2, \ldots, xn)$. It is noted that a matrix of N_p is randomly initialized. They are regarded as the test points which are located in the cloud and the ground surface [54, 58, 59]. The test points can be defined as

$$x_{\text{testpoint}}^i = x_{\min}^i + \left(x_{\max}^i - x_{\min}^i\right) \times \text{rand}[0, 1] \tag{15}$$

where $x_{\min}^i$ and $x_{\max}^i$ denote the upper and lower bounds of design variables. Rank is a randomly given parameter in range from zero to one. Fitness of the solution is defined as

$$F_{\text{testpoint}}^i = \text{obj}\left(x_{\text{testpoint}}^i\right). \tag{16}$$

Step 2 Next jump determination

Herein, the test points in vector $x_{\text{testpoint}}^i$ achieve a high value of electrical field which is considered as the potential next jump points. Assume that the point k is chosen from the population. If the electric field of point k (the fitness of point k) is better than that of the averages of all test points, the tendency of lightning jumps toward this point. Otherwise, the

lightning displaces to other direction. After that, the average value of the overall test points and the value of fitness of the points are computed as in Eqs. (17)–(18), respectively.

$$x_{\text{average}} = \text{mean}\left(x_{\text{testpoint}}\right), \tag{17}$$

$$f_{\text{average}} = \text{obj}\left(x_{\text{average}}\right), \tag{18}$$

where x_{average} and f_{average} note the average value and value of fitness of the points, respectively.

If the electric field, fitness function, of potential point h is greater than the average value of the test points, it is calculated as

$$x^i_{\text{testpoint\_new}} = x^i_{\text{testpoint}} + \text{rand}[0,\,1] \times \left(x_{\text{average}} + \text{rand}[0,\,1] \times \left(x^h_{\text{potential point}}\right)\right). \tag{19}$$

Otherwise, it is calculated as

$$x^i_{\text{testpoint\_new}} = x^i_{\text{testpoint}} - \text{rand}[0,\,1] \times \left(x_{\text{average}} + \text{rand}[0,\,1] \times \left(x^h_{\text{potential point}}\right)\right). \tag{20}$$

Step 3 Branch fading

If the fitness function of new test point ($x^i_{\text{testpoint\_new}}$) is better than the previous point ($x^i_{\text{testpoint}}$), the branch sustains; otherwise, the branch fades as

$$\begin{aligned} x^i_{\text{testpoint}} &= x^i_{\text{testpoint\_new}}, \quad f^i_{\text{testpoint\_new}} < f^i_{\text{testpoint}} \\ x^i_{\text{testpoint\_}new} &= x^i_{\text{testpoint}}, \quad \text{otherwise.} \end{aligned} \tag{21}$$

This step is carried out for overall the test points so as to rest points moving down.

Step 4 Upward leader movement

In this step, an exponent factor based on the charge of downward leader is employed to take all the test points as the upward leader and moved up. The exponent factor is based on the charge of downward leader, which can be defined by

$$S = 1 - \frac{noi}{noi_{\max}} \times \exp\left(-\frac{noi}{noi_{\max}}\right), \tag{22}$$

where noi and $noi_{\max}$ denote the number of iterations and maximum number of iterations, respectively. The upward leaders are defined for the next strategy of test point as

$$x_{\text{testpoint\_new}} = x_{\text{testpoint\_new}} + \text{rand}[0,\,1] \times S\left(x_{\min} - x_{\max}\right), \tag{23}$$

where $x_{\min}$ and $x_{\max}$ denote the best value and the worst solution of the population, respectively.

In each iteration, it should be remarked that the average of the entire population is computed by Eq. (17). The fitness of the average solution is determined by Eq. (18). If the fitness of the worst solution is worse than the average one, it is updated by the average solution.

Step 5 Final jump

The process is ended when the upward leader meets the downward leader to each other. It is noted that the optimization process is ended if stop criterion is achieved. In addition, the maximum iteration is met and the process is ended herein. In this paper, the maximum iteration is chosen as 10^4.

3 Case Studies: MOO Design for Bridge Amplification Mechanism

In order to effectively solve a MOO design of bridge amplification mechanism (BAM), this article considers three numerical examples. The obtained results from these numerical solutions also evaluate application's capability and effectiveness of the proposed hybrid methodology.

3.1 Structural Description

Figure 3 demonstrates a mechanical structure of the BAM. The bottom end of the BAM is located at fixed supports by screws, while the top end is moved freely. This mechanism includes four flexure hinges at the top side and four flexure hinges at bottom side, which is arranged in a symmetric configuration, as shown in Fig. 3a. The BAM consists of a rigid link 2 coupled with two rigid links 1 through flexure hinges. The output, such called end effector, is at the middle of rigid link 2. Based on symmetric topology, the output of mechanism can move along the y-axis by exciting two input loads from piezoelectric actuators, as depicted in Fig. 3b. The purposes of the BAM do not amplify a large working stroke along the desired direction but also ensure a high safety factor. The mechanism includes main parameters such as $H, H_1, H_2, H_3, H_4, L, L_1, L_2, L_3, T, W, W_1$, and W_2, as given in Figs. 3 and 4. In this article, AL T73-7075 material is chosen for the mechanism because of its lightweight. According to mechanic theory of bistable compliant mechanisms and others [60, 61], the main design parameters are comprised of structural parameters being considered as a vector of design variable $\mathbf{X} = [L_1, L_2, L_3, H_1, H_2, T]^{\text{T}}$. Remain parameters (W, H, L, H_3, H_4) are assigned as constant values.

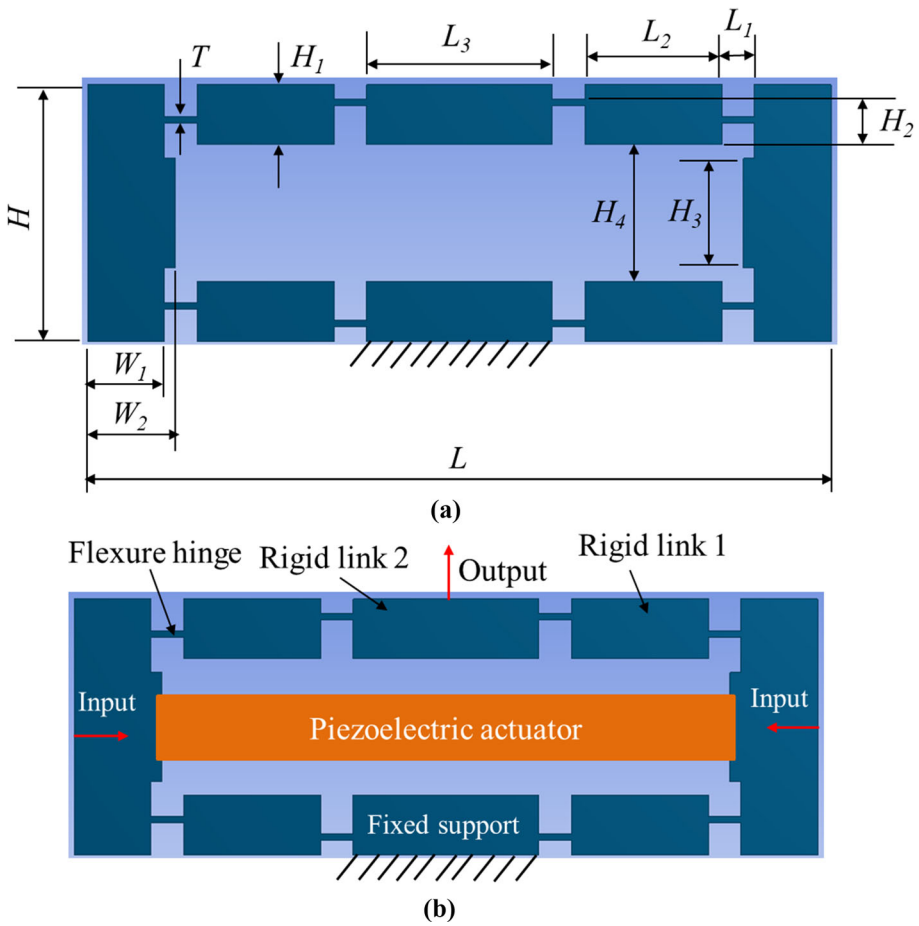

Fig. 3 Schematics of the bridge amplification mechanism (unit: mm): **a** dimension, **b** working principle

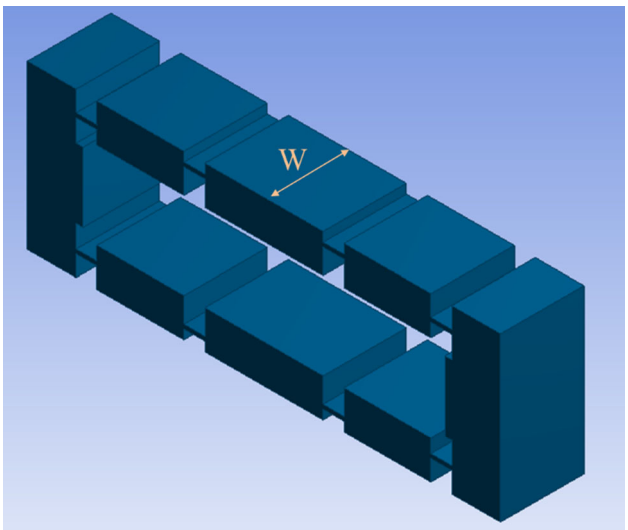

Fig. 4 3D model of the bridge amplification mechanism (unit: mm)

Table 1 gives the geometrical parameters of the proposed BAM and the mechanical properties of AL T73-7075 material. The ranges of upper and lower bounds of design variables are determined based on a capacity of fabrication device.

3.2 Numerical Simulation

A 3D FEM model is created, and then, the numerical experiments are formulated via the BBD. Numerical data are then collected by implementing FEA simulations. The boundary conditions and loads are given, as shown in Fig. 3. A load of 0.08 mm is applied to both sides of inputs of the mechanism along the horizontal direction. Meanwhile, the output response of the mechanism is amplified along the vertical direction. Sizing technique is utilized for meshing. Meshing of flexure hinges is refined in order to achieve accurate analysis, as shown in Fig. 5. The meshing results give a number of elements of 8155 and a number of nodes of 16379. Skewness criteria, metric performance, are used to evaluate the quality of meshing. Its value is in the range from zero to one. The results showed that the average value of skewness is approximately 0.60619. In the other word, this value guarantees the quality of meshing is relatively good, as given in Fig. 6.

Table 1 Geometrical parameters and material properties of bridge amplification compliant mechanism

Design parameters	Symbol	Value
Length of flexure hinge	L_1	11.25 mm $\leq L_1 \leq$ 13.75 mm
Length of rigid link 1	L_2	2.7 mm $\leq L_2 \leq$ 3.3 mm
Length of rigid link 2	L_3	16.7 mm $\leq L_3 \leq$ 18.7 mm
Thickness of rigid links	H_1	4.5 mm $\leq H_1 \leq$ 6.5 mm
Distance between two flexure hinges	H_2	1.5 mm $\leq H_2 \leq$ 1.7 mm
Thickness of flexure hinges	T	0.45 mm $\leq T \leq$ 0.65 mm
Height of input link	H_3	10 mm
Distance between upper and lower series	H_4	12.25 mm
First width of input link	W_1	7 mm
Second width of input link	W_2	8 mm
Width of the mechanism	W	10 mm
Height of the mechanism	H	24 mm
Length of the mechanism	L	68 mm
Total size of the mechanism		68 × 24 × 10 mm^3
Mechanical properties of Al T73-7075		
Density		2810 kg/m^3
Young's modulus		71700 MPa
Yield strength		503 MPa
Poisson's ratio		0.33

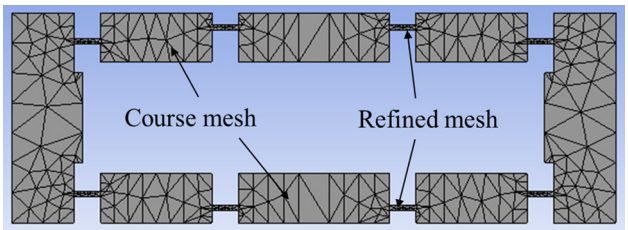

Fig. 5 Meshing model of the bridge amplification mechanism

Table 2 Levels of their design variables

Symbol	Value	Level 1	Level 2	Level 3
L_1	2.7 mm $\leq L_1 \leq$ 3.3 mm	11.25	12.50	13.75
L_2	11.25 mm $\leq L_2 \leq$ 13.75 mm	2.7	3.0	3.3
L_3	16.7 mm $\leq L_3 \leq$ 18.7 mm	16.7	17.7	18.7
H_1	4.5 mm $\leq H_1 \leq$ 6.5 mm	4.5	5.5	6.5
H_2	1.5 mm $\leq H_2 \leq$ 1.7 mm	1.44	1.6	1.76
T	0.45 mm $\leq T \leq$ 0.65 mm	0.45	0.55	0.66

4 Results and Discussion

4.1 Sensitivity Investigation and Refinement of Design Variables

In order to decrease the complexity of the proposed algorithm, a whole of initial design variables are evaluated to reduce the searching space. The goal of sensitivity analysis is to redetermine a few populations for the further LAPO algorithm. This section firstly determines the most critical important parameters and the nonsignificant ones. Secondly, it refines space of design variables. In this article, six factors are divided into three levels, as given in Table 2. Each numerical experiment retrieves two quality specifications and one constraint, including safety factor (F_1 (**X**) and displacement (F_2 (**X**)-mm), and equivalent stress (F_3 (**X**)-MPa). Forty-nine experiments are generated and the numerical results are given, as shown in Table 3.

As stated above, this article considers two objective functions. Furthermore, it considers two constraints for two objective functions and one constraint about working strength for solving MOO problem of the BAM. The sensitivity of design variables with respect to the displacement, safety factor, and stress is analyzed, individually. In this study, ANOVA and Taguchi approach are implemented by using Minitab software 18.

Case study 1 considers the safety factor. ANOVA is utilized for analysis of sensitivity at 95% confidence interval. The results in Table 4 show that the contribution of parameters L_1, L_3, and H_1 on the safety factor is about 0% with p

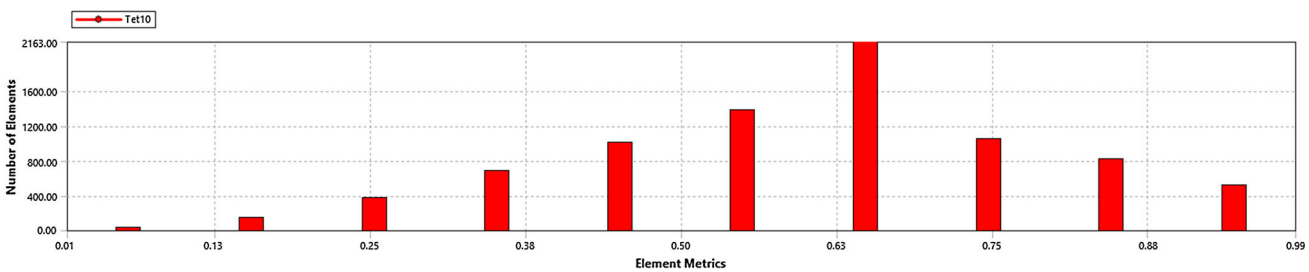

Fig. 6 Quality of meshing elements using Skewness criterion

Table 3 Initially numerical results: safety factor, displacement, and stress

No.	Design variables (Unit: mm)						Safety factor	Displacement	Stress
1	L_1	L_2	L_3	T	H_1	H_2	F_1 (**X**)	F_2 (**X**)-mm	F_3 (**X**)-MPa
2	3	12.5	16.85	0.555	5.5	1.6	1.472587573	1.426138043	341.5756109
3	2.7	11.25	16.85	0.45	5.5	1.6	1.60331877	1.324164271	313.7242633
4	2.7	13.75	16.85	0.45	5.5	1.6	1.609474228	1.560522676	312.5244203
5	3.3	11.25	16.85	0.45	5.5	1.6	1.923061347	1.386443853	261.5621186
6	3.3	13.75	16.85	0.45	5.5	1.6	1.914484932	1.622220874	262.7338516
7	2.7	11.25	16.85	0.66	5.5	1.6	1.216333723	1.229423761	413.5378231
8	2.7	13.75	16.85	0.66	5.5	1.6	1.208586433	1.445500851	416.1886864
9	3.3	11.25	16.85	0.66	5.5	1.6	1.414269143	1.293904662	355.660733
10	3.3	13.75	16.85	0.66	5.5	1.6	1.394503216	1.511931181	360.701929
11	2.7	12.5	15	0.555	4.5	1.6	1.373567166	1.389369249	366.1997843
12	3.3	12.5	15	0.555	4.5	1.6	1.645083955	1.456207037	305.7594711
13	2.7	12.5	18.7	0.555	4.5	1.6	1.397360273	1.386978626	359.9644343
14	3.3	12.5	18.7	0.555	4.5	1.6	1.639985447	1.454615116	306.7100387
15	2.7	12.5	15	0.555	6.5	1.6	1.363312698	1.397742271	368.9542397
16	3.3	12.5	15	0.555	6.5	1.6	1.612947701	1.463092089	311.8514008
17	2.7	12.5	18.7	0.555	6.5	1.6	1.354836488	1.395954967	371.2625135
18	3.3	12.5	18.7	0.555	6.5	1.6	1.593021891	1.459637046	315.7520953
19	3	12.5	15	0.45	5.5	1.44	1.586714944	1.617383003	317.0071613
20	3	12.5	18.7	0.45	5.5	1.44	1.582628352	1.617017269	317.8257228
21	3	12.5	15	0.66	5.5	1.44	1.191600207	1.48103106	422.1214441
22	3	12.5	18.7	0.66	5.5	1.44	1.198413863	1.479096889	419.7214465
23	3	12.5	15	0.45	5.5	1.76	1.933504622	1.350423336	260.1493651
24	3	12.5	18.7	0.45	5.5	1.76	1.919370206	1.35050714	262.0651287
25	3	12.5	15	0.66	5.5	1.76	1.452630765	1.273059964	346.26831
26	3	12.5	18.7	0.66	5.5	1.76	1.416643905	1.269780993	355.0645283
27	3	11.25	16.85	0.45	4.5	1.6	1.781452363	1.353460312	282.3538875
28	3	13.75	16.85	0.45	4.5	1.6	1.785040587	1.588487983	281.7863098
29	3	11.25	16.85	0.66	4.5	1.6	1.330082409	1.255393028	378.1720565
30	3	13.75	16.85	0.66	4.5	1.6	1.341285713	1.469329	375.0133137
31	3	11.25	16.85	0.45	6.5	1.6	1.740143667	1.356318355	289.0565931
32	3	13.75	16.85	0.45	6.5	1.6	1.749753525	1.591756463	287.4690594
33	3	11.25	16.85	0.66	6.5	1.6	1.314709609	1.264823675	382.5939939
34	3	13.75	16.85	0.66	6.5	1.6	1.298884546	1.482865691	387.2553583
35	2.7	12.5	16.85	0.555	4.5	1.44	1.249208107	1.512535334	402.6550877
36	3.3	12.5	16.85	0.555	4.5	1.44	1.484492527	1.587330222	338.8363302
37	2.7	12.5	16.85	0.555	6.5	1.44	1.225446798	1.521378517	410.4625356
38	3.3	12.5	16.85	0.555	6.5	1.44	1.459963278	1.592926264	344.5292135
39	2.7	12.5	16.85	0.555	4.5	1.76	1.491748181	1.280308843	337.1882777
40	3.3	12.5	16.85	0.555	4.5	1.76	1.79908385	1.342087269	279.5867463
41	2.7	12.5	16.85	0.555	6.5	1.76	1.464464162	1.287930727	343.4703376
42	3.3	12.5	16.85	0.555	6.5	1.76	1.752125826	1.344850659	287.0798389
43	3	11.25	15	0.555	5.5	1.44	1.334165268	1.432215571	377.0147612
44	3	13.75	15	0.555	5.5	1.44	1.340641395	1.679494023	375.1935469
45	3	11.25	18.7	0.555	5.5	1.44	1.341636769	1.431200266	374.9151868
46	3	13.75	18.7	0.555	5.5	1.44	1.344417618	1.678059101	374.1396967
47	3	11.25	15	0.555	5.5	1.76	1.601065157	1.20985055	314.1658526
48	3	13.75	15	0.555	5.5	1.76	1.620710078	1.421619892	310.3577912
49	3	11.25	18.7	0.555	5.5	1.76	1.635506916	1.211179018	307.5499071
	3	13.75	18.7	0.555	5.5	1.76	1.644002476	1.420678973	305.9606098

Table 4 ANOVA results for the safety factor

Source	*DF*	Seq SS	Contribution (%)	Adj SS	Adj MS	*F* value	*p* value
Model	21	2.08824	98.45	2.08824	0.09944	81.70	0.000
Linear	6	2.07271	97.72	2.07271	0.34545	283.84	0.000
L_1	1	0.00001	0.00	0.00001	0.00001	0.01	0.926
L_2	1	0.39408	18.58	0.39408	0.39408	323.79	0.000
L_3	1	0.00001	0.00	0.00001	0.00001	0.00	0.945
T	1	1.19305	56.25	1.19305	1.19305	980.26	0.000
H_1	1	0.00630	0.30	0.00630	0.00630	5.17	0.031
H_2	1	0.47927	22.60	0.47927	0.47927	393.79	0.000
Two-way interaction	15	0.01552	0.73	0.01552	0.00103	0.85	0.620
$L_1 * L_2$	1	0.00009	0.00	0.00009	0.00009	0.07	0.788
$L_1 * L_3$	1	0.00003	0.00	0.00003	0.00003	0.02	0.882
$L_1 * T$	1	0.00012	0.01	0.00012	0.00012	0.09	0.761
$L_1 * H_1$	1	0.00006	0.00	0.00006	0.00006	0.05	0.833
$L_1 * H_2$	1	0.00004	0.00	0.00004	0.00004	0.04	0.850
$L_2 * L_3$	1	0.00020	0.01	0.00020	0.00020	0.17	0.686
$L_2 * T$	1	0.00725	0.34	0.00725	0.00725	5.96	0.021
$L_2 * H_1$	1	0.00014	0.01	0.00014	0.00014	0.11	0.740
$L_2 * H_2$	1	0.00196	0.09	0.00196	0.00196	1.61	0.215
$L_3 * T$	1	0.00001	0.00	0.00001	0.00001	0.01	0.912
$L_3 * H_1$	1	0.00028	0.01	0.00028	0.00028	0.23	0.637
$L_3 * H_2$	1	0.00000	0.00	0.00000	0.00000	0.00	0.964
$T * H_1$	1	0.00004	0.00	0.00004	0.00004	0.04	0.850
$T * H_2$	1	0.00522	0.25	0.00522	0.00522	4.29	0.048
$H_1 * H_2$	1	0.00008	0.00	0.00008	0.00008	0.07	0.795
Error	27	0.03286	1.55	0.03286	0.00122		
Total	48	2.12110	100.00				

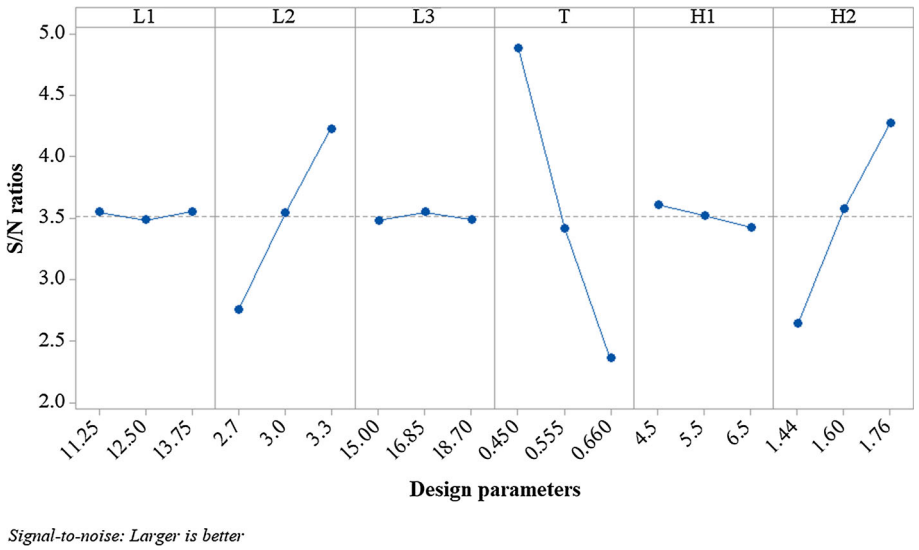

Fig. 7 Effect plot of design variables on the safety factor

value of 0.926, 0.945, and 0.031, respectively. These p values are more than 0.5%. According to the statistical theory, p value is less than 0.5%, and that parameter is significant. It means that the contributions of L_1, L_3, and H_1 are very small and can be ignored in further modeling and optimization process. In addition, the Taguchi method with larger-the-better type is used for this response to describe influencing plot of displacement, as shown in Fig. 7. The results also showed that

Table 5 ANOVA results for the displacement

Source	*DF*	Seq SS	Contribution (%)	Adj SS	Adj MS	*F* value	*p* value
Model	21	0.746943	99.78	0.746943	0.035569	587.73	0.000
Linear	6	0.744068	99.40	0.744068	0.124011	2049.13	0.000
L_1	1	0.309194	41.30	0.309194	0.309194	5109.04	0.000
L_2	1	0.025574	3.42	0.025574	0.025574	422.58	0.000
L_3	1	0.000012	0.00	0.000012	0.000012	0.19	0.663
T	1	0.066420	8.87	0.066420	0.066420	1097.50	0.000
H_1	1	0.000288	0.04	0.000288	0.000288	4.76	0.038
H_2	1	0.342580	45.76	0.342580	0.342580	5660.71	0.000
Two-way interaction	15	0.002875	0.38	0.002875	0.000192	3.17	0.004
$L_1 * L_2$	1	0.000000	0.00	0.000000	0.000000	0.00	0.951
$L_1 * L_3$	1	0.000001	0.00	0.000001	0.000001	0.01	0.904
$L_1 * T$	1	0.000366	0.05	0.000366	0.000366	6.05	0.021
$L_1 * H_1$	1	0.000003	0.00	0.000003	0.000003	0.04	0.839
$L_1 * H_2$	1	0.000664	0.09	0.000664	0.000664	10.97	0.003
$L_2 * L_3$	1	0.000000	0.00	0.000000	0.000000	0.00	0.969
$L_2 * T$	1	0.000006	0.00	0.000006	0.000006	0.10	0.755
$L_2 * H_1$	1	0.000011	0.00	0.000011	0.000011	0.19	0.667
$L_2 * H_2$	1	0.000096	0.01	0.000096	0.000096	1.58	0.220
$L_3 * T$	1	0.000003	0.00	0.000003	0.000003	0.05	0.824
$L_3 * H_1$	1	0.000000	0.00	0.000000	0.000000	0.00	0.955
$L_3 * H_2$	1	0.000000	0.00	0.000000	0.000000	0.00	0.951
$T * H_1$	1	0.000035	0.00	0.000035	0.000035	0.59	0.451
$T * H_2$	1	0.001687	0.23	0.001687	0.001687	27.88	0.000
$H_1 * H_2$	1	0.000002	0.00	0.000002	0.000002	0.03	0.855
Error	27	0.001634	0.22	0.001634	0.000061		
Total	48	0.748577	100.00				

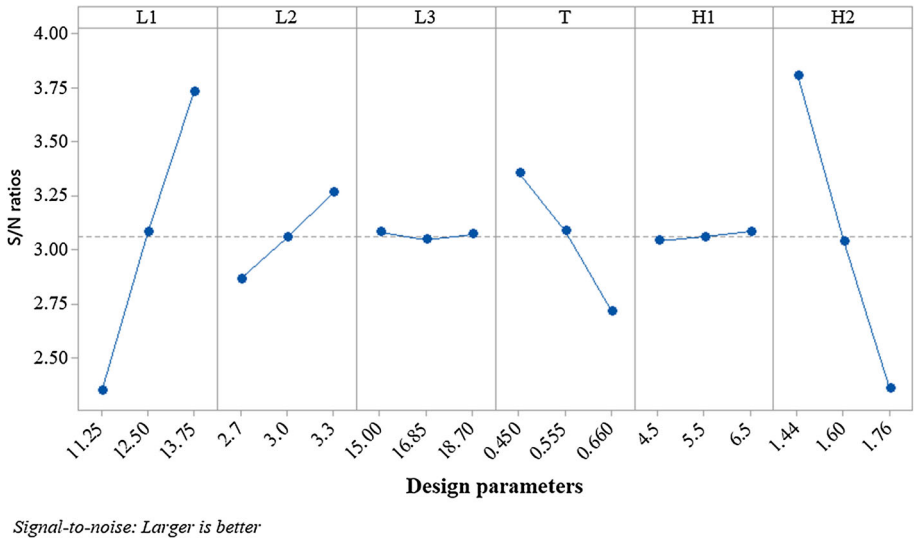

Fig. 8 Effect plot of design variables on the displacement

factors L_1, L_3, and H_1 are two nonsignificant factors because the safety factor is a little change when those parameters are varied. Meanwhile, other parameters are very sensitive to the safety factor which are taken as key variables for case study 1.

Considering the displacement, case study 2 is expected to be the higher-the-better type. In Table 5, the ANOVA results revealed that parameters L_3 and H_1 have a lowest contribution on the displacement with respect to 0.663% and 0.038%, respectively. These *p* values are larger than 0.5%. As a result,

Table 6 ANOVA results for the equivalent stress

Source	*DF*	Seq SS	Contribution (%)	Adj SS	Adj MS	*F* value	*p* value
Model	27	101509	99.82	101509	3759.6	435.64	0.000
Linear	6	100753	99.08	100753	16792.1	1945.80	0.000
L_1	1	0	0.00	0	0.0	0.00	0.946
L_2	1	19572	19.25	19572	19572.1	2267.93	0.000
L_3	1	1	0.00	1	0.7	0.08	0.778
T	1	56458	55.52	56458	56458.0	6542.12	0.000
H_1	1	305	0.30	305	304.7	35.30	0.000
H_2	1	24417	24.01	24417	24417.2	2829.37	0.000
Square	6	561	0.55	561	93.5	10.83	0.000
$L_1 * L_1$	1	59	0.06	1	1.0	0.12	0.733
$L_2 * L_2$	1	13	0.01	9	8.5	0.99	0.332
$L_3 * L_3$	1	31	0.03	15	15.1	1.75	0.200
$T * T$	1	255	0.25	149	149.4	17.32	0.000
$H_1 * H_1$	1	157	0.15	43	42.6	4.94	0.037
$H_2 * H_2$	1	47	0.05	47	46.6	5.40	0.030
Two-way interaction	15	195	0.19	195	13.0	1.51	0.190
$L_1 * L_2$	1	3	0.00	3	2.8	0.33	0.573
$L_1 * L_3$	1	1	0.00	1	1.3	0.15	0.698
$L_1 * T$	1	8	0.01	8	8.1	0.94	0.344
$L_1 * H_1$	1	6	0.01	6	5.8	0.67	0.422
$L_1 * H_2$	1	1	0.00	1	1.0	0.11	0.739
$L_2 * L_3$	1	10	0.01	10	9.6	1.12	0.303
$L_2 * T$	1	16	0.02	16	16.3	1.89	0.184
$L_2 * H_1$	1	0	0.00	0	0.0	0.00	0.988
$L_2 * H_2$	1	31	0.03	31	31.0	3.60	0.072
$L_3 * T$	1	2	0.00	2	1.7	0.19	0.664
$L_3 * H_1$	1	17	0.02	17	16.5	1.91	0.181
$L_3 * H_2$	1	1	0.00	1	1.2	0.14	0.710
$T * H_1$	1	2	0.00	2	2.3	0.27	0.612
$T * H_2$	1	97	0.10	97	97.2	11.27	0.003
$H_1 * H_2$	1	0	0.00	0	0.0	0.00	0.974
Error	21	181	0.18	181	8.6		
Total	48	101690	100.00				

the factors L_3 and H_1 are nonsignificant variables that can be neglected in modeling and optimization process for case study 2.

Figure 8 describes the sensitivity of full variables on the displacement via using the Taguchi method. It also notes that the parameters L_3 and H_1 have a very small influence on this response. On the other hand, if these parameters are varied, the displacement is somehow changed. When there is any a change in the remain parameters, the displacement has a sharply change.

Case study 3 deals with the equivalent stress, the ANOVA results in Table 6 indicated that three parameters L_1 and L_3 have the lowest contribution on the stress with p value of 0.946 and 0.778, respectively. These values are more than 0.5%. According to the statistical theory, such factors are nonsignificant and can be suppressed in further modeling and the MOO process. A smaller-the-better type is utilized for the stress. The results the Taguchi analysis show that three parameters L_1 and L_3 also have a very small contribution on the stress response, as shown in Fig. 9.

4.2 Optimization Implementation

4.2.1 Selection of Membership Functions

In this section, the desirability values of both displacement and the safety factor of the BAM are calculated, and their results transformed into the FIS. The desirability values of

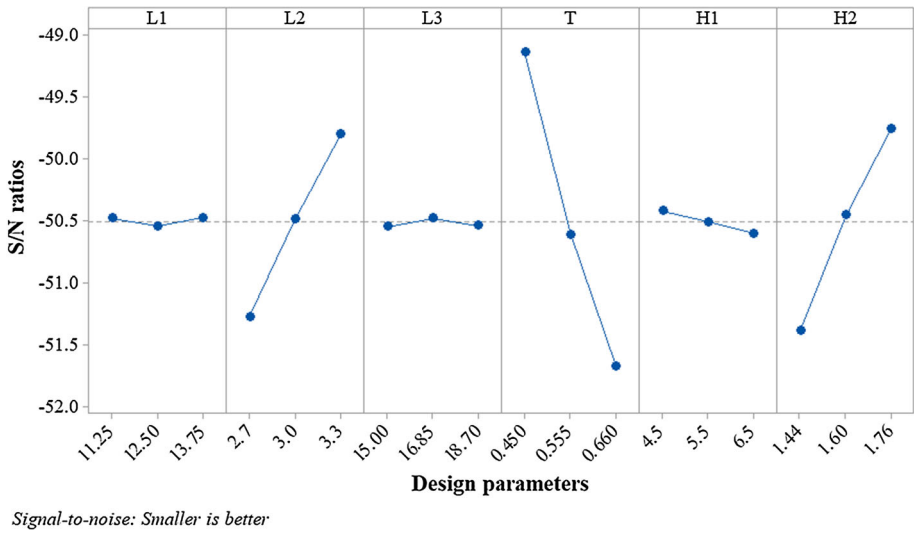

Fig. 9 Effect plot of design variables on the stress

Table 7 Linguistic variables for fuzzy reasoning process

Symbol	T	VS	S	SM	M	ML	L	VL	H
Linguistic variables	Tiny	Very small	Small	Small–medium	Medium	Medium–large	Large	Very large	Huge

both displacement and the safety factor are assigned as two inputs for the FIS. Two inputs and one output (MPCI) of this system are fuzzed by assigning the linguistic variables. Table 7 shows the linguistic variables, including tiny, very small, small, small–medium, medium, medium–large, large, very large, and huge.

The MFs for desirability of safety factor are divided into three levels such as small, medium, and large, as illustrated in Fig. 10a. Meanwhile, the MFs of the desirability of displacement are separated into seven levels, including tiny, very small, small–medium, medium, medium–large, large, very large, and huge, as depicted in Fig. 10b. At last, the MFs of the output MPCI also include seven levels, as shown in Fig. 11. All the MFs are defined by trapezoidal shape because this is a popular MFs type for both the FIS and ANFIS model.

The results of sensitivity analysis help to decrease computational time. Particularly, some parameters may be redundant, while others are critically important factors. In the other word, a sensitivity research is needed to refine a space of design variables. Based on the sensitivity results, three following numerical examples are considered to evaluate the performance effectiveness of proposed methodology. Aforementioned above, a general optimization problem of the BAM is briefly stated as follows:

Find vector of design variable: $\mathbf{X} = [L_1, L_2, L_3, H_1, H_2, T]^{\mathrm{T}}$

$$\text{Maximize} \quad F_1(\mathbf{X}) \tag{24}$$

$$\text{Maximixe} \quad F_2(\mathbf{X}) \tag{25}$$

Subject to constraints:

$$\begin{aligned} F_1(\mathbf{X}) &\geq 1.5 \\ F_2(\mathbf{X}) &\geq 1.7\,\text{mm} \\ F_3(\mathbf{X}) &\leq \sigma_a \end{aligned} \tag{26}$$

Initial space of design variables:

$$\begin{aligned} 2.7\,\text{mm} &\leq L_1 \leq 3.3\,\text{mm} \\ 11.25\,\text{mm} &\leq L_2 \leq 13.75\,\text{mm} \\ 16.7\,\text{mm} &\leq L_3 \leq 18.7\,\text{mm} \\ 4.5\,\text{mm} &\leq H_1 \leq 6.5\,\text{mm} \\ 1.44\,\text{mm} &\leq H_2 \leq 1.76\,\text{mm} \\ 0.45\,\text{mm} &\leq T \leq 0.65\,\text{mm} \end{aligned} \tag{27}$$

where F_1 (**X**), F_2 (**X**), and F_3 (**X**) denote the safety factor, displacement, and stress, respectively. σ_a is the yield stress of proposed Al T73-7075. Specifically, F_1 (**X**) and F_2 (**X**) are two objective functions, while F_3 (**X**) is regarded as the constraint.

If the full initial space is used, it may take a long time to search optimum solutions. Therefore, this study limits the searching spaces in Eq. (27). The following case studies are separated to investigate and evaluate the efficiency of proposed hybrid approach.

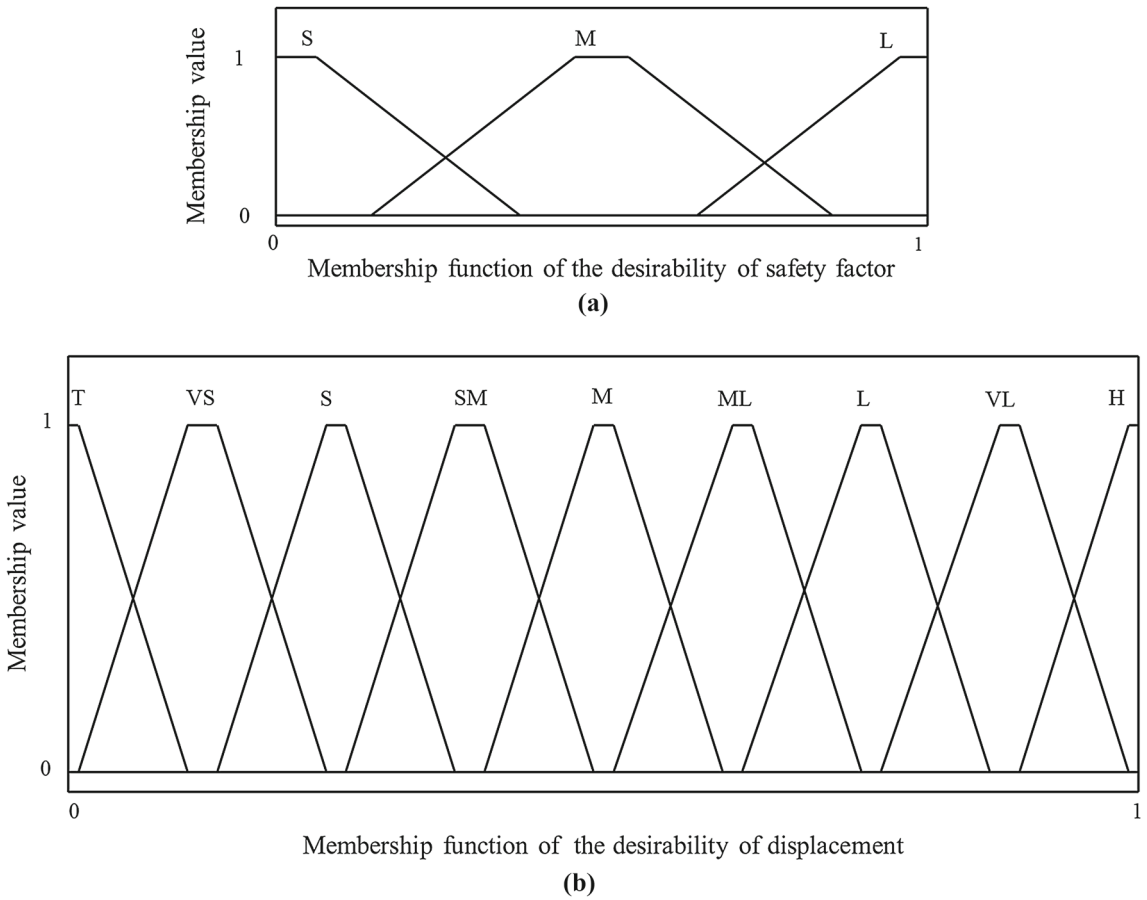

Fig. 10 Membership functions plot: **a** the safety factor and **b** the displacement

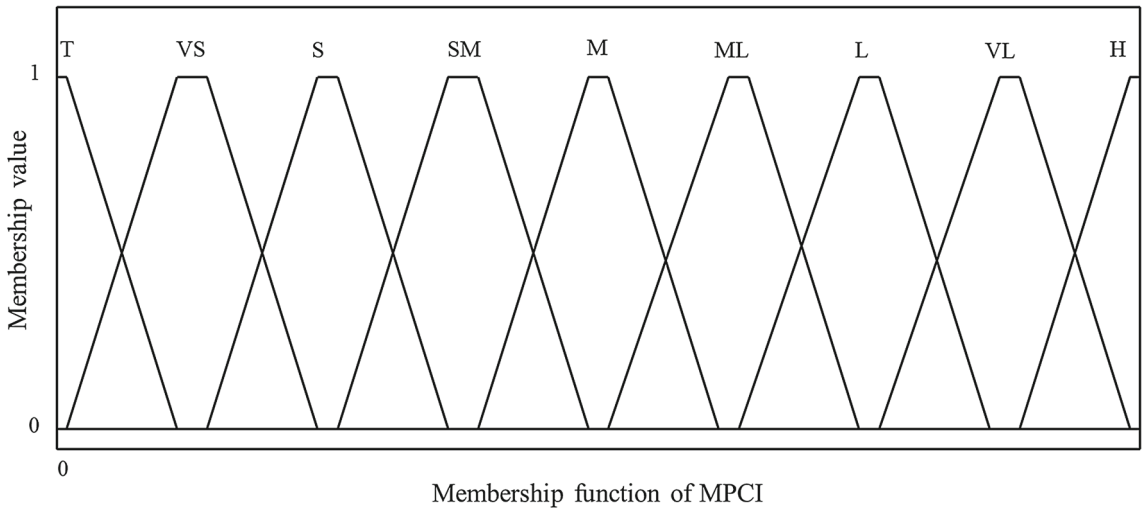

Fig. 11 Membership functions plot for the MPCI

4.2.2 Case Study 1

Based on the results of sensitivity analysis in Table 4 and Fig. 7, the lowest contributing factors are suppressed during the optimization process since their influences are very small on the safety factor. Meanwhile, real influencing factors with large contributions are taken into account as key design variables. Case study 1 takes two objective functions to be optimized simultaneously with the spaces of design variables are relatively reduced. In order to solve MOO problem,

Table 8 Desirability results of the case study 1

No.	Design variables (unit: mm)			Safety factor	Displacement	Stress	Desirability of safety factor	Desirability of displacement
	L_2	T	H_2	F_1 (**X**)	F_2 (**X**)-mm	F_3 (**X**)-MPa	d_1	d_2
1	12.5	0.555	1.6	1.475086	1.425435	340.9972	0.380999704	0.459061168
2	11.25	0.45	1.6	1.753896	1.354951	286.7901	0.761457884	0.310888149
3	13.75	0.45	1.6	1.774099	1.591645	283.5242	0.785413035	0.818092581
4	11.25	0.66	1.6	1.319707	1.263442	381.1451	0.172242603	0.109036186
5	13.75	0.66	1.6	1.314954	1.480399	382.523	0.162202839	0.574090949
6	11.25	0.555	1.44	1.333424	1.43232	377.2244	0.185263001	0.473312026
7	13.75	0.555	1.44	1.335427	1.678723	376.6585	0.191556403	0.997841414
8	11.25	0.555	1.76	1.620762	1.210485	310.3479	0.578640577	0.002158586
9	13.75	0.555	1.76	1.623741	1.420928	309.7785	0.586262563	0.449888393
10	12.5	0.45	1.44	1.583884	1.618079	317.5738	0.531301625	0.868582001
11	12.5	0.66	1.44	1.195386	1.480652	420.7844	0	0.581500805
12	12.5	0.45	1.76	1.929505	1.35067	260.6886	1	0.294874372
13	12.5	0.66	1.76	1.431208	1.273322	351.4514	0.319130754	0.136101974

the desirability of safety factor and the desirability of displacement are transformed into a single combined objective function, which is called as the MPCI of the FIS. According to the fuzzy theory [34], the MPCI should be maximized to reach an optimal solution. The optimization problem of case study 1 is stated as follows:

Find vector of design variable: $\mathbf{X} = [L_2, T, H_2]^{\mathrm{T}}$

$$\text{Maximize} \quad \text{MPCI}(\mathbf{X})_{\text{case study 1}} \tag{28}$$

S.t.

$$\begin{aligned} F_1(\mathbf{X}) &\geq 1.5 \\ F_2(\mathbf{X}) &\geq 1.7 \text{ mm} \\ F_3(\mathbf{X}) &\leq \sigma_a \\ 11.25 \text{ mm} \leq L_2 &\leq 13.75 \text{ mm} \\ 0.45 \text{ mm} \leq T &\leq 0.66 \text{ mm} \\ 1.44 \text{ mm} \leq H_2 &\leq 1.76 \text{ mm} \end{aligned} \tag{29}$$

Case study 1 evaluates three design variables (L_2, T, and H_1) and two objective functions and three constraints. Based on the number of design variables and their levels, BBD is used to build 13 experiments. The results of displacement, safety factor, and stress are collected, simultaneously.

Next, desirability of safety factor and desirability of displacement are calculated, as given in Table 8. Real values of two responses have different units, and it is a main cause resulting in un-precise solutions. Therefore, desirability function approach is proposed to overcome this limitation because desirability has no unit and its value from zero to one. The results showed all stress values are satisfied in terms of allowable stress of material.

In order to conduct the MOO problem for case study 1, the MFs for desirability of safety factor include three levels and the ones of displacement are divided into seven levels, while the MFs of fuzzy MPCI output are separated into seven levels, as given in Table 9. Subsequently, matrix of fuzzy rules is built in this table.

In this study, center of gravity method is employed for defuzzification and Mamdani method is utilized for fuzzy operation. The FIS is implemented in MATLAB R2019b. Figure 12 illustrates a relation of the fuzzy MPCI with the desirability of safety factor and desirability of displacement. The value of inputs and outputs of the FIS are in range from zero to one. In this study, the weight of each rule is assumed to be unity.

Based on 27 fuzzy rules in Table 9, the output of FIS is computed, as shown in Fig. 13.

The results of MPCI output are determined with respect to each value of desirability of displacement and desirability of safety factor, as given in Table 10.

By taking the values of design variables in Table 8 and the MPCI value in Table 10, a proper ANFIS model is developed for modeling the MPCI. Modeling is coded in MATLAB R2019b. The predicting accuracy of the develop ANFIS models for three case studies is evaluated through the root mean square error (RMSE) and coefficient of determination (R^2) [62]. The results of ANFIS parameters are given in Table 11.

According to the theory of fuzzy logic [34], in order to get a large displacement and a high safety factor simultaneously, a larger-the-better value is desired for the MPCI. In the other word, the MPCI must be maximized so as to achieve

Table 9 Fuzzy rules matrix for case study 1

No.	Desirability for F_1 (**X**)	Desirability for F_2 (**X**)	MPCI
1	S	T	T
2	M	T	VS
3	L	T	S
4	S	VS	VS
5	M	VS	S
6	L	VS	SM
7	S	S	S
8	M	S	SM
9	L	S	ML
10	S	SM	S
11	M	SM	SM
12	L	SM	M
13	S	M	SM
14	M	M	M
15	L	M	ML
16	S	ML	SM
17	M	ML	M
18	L	ML	ML
19	S	L	ML
20	M	L	ML
21	L	L	L
22	S	VL	ML
23	M	VL	L
24	L	VL	VL
25	S	H	ML
26	M	H	L
27	L	H	H

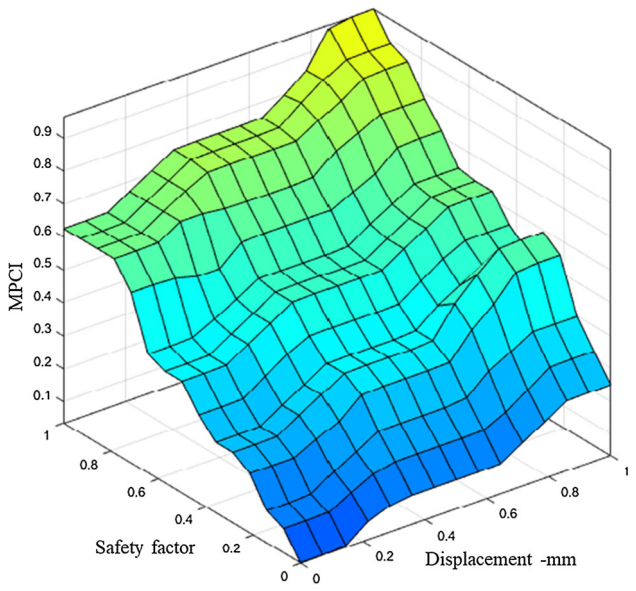

Fig. 12 Plot of input versus output in the FIS

a global optimal solution. In order to evaluate the effectiveness and robustness of the proposed hybrid approach, the optimal results are compared with those obtained from a traditional combination of the Taguchi method and fuzzy logic (TMFL), the optimal results from the TMFL are determined at $L_2 = 13.75$ mm, $T = 0.45$ mm, and $H_2 = 1.44$ mm, as given in Table 12. The results of TMFL find that the optimal displacement and the optimal safety factor are approximately 1.74598 mm and 1.59843, respectively. However, those optimal values are discrete points. Such points can lead to local optimum solutions. To overcome this limitation, LAPO algorithm is used to search a global optimum solution. Based on the established ANFIS modeling, a pseudo-objective function of MPCI is well established. And then, a LAPO programming is implemented in MATLAB R2019b, and the results of the proposed approach showed that the optimal design parameters are at $L_2 = 13.80$ mm, $T = 0.50$ mm, and $H_2 = 1.44$ mm. By using the proposed methodology, the optimal displacement and the optimal safety factor are found at 1.7686 mm and 11.5111, respectively. Besides, the optimal MPCI predicted from the TMFL is smaller than that predicted from the proposed hybrid methodology. According to a larger-the-better value is best for the MPCI, the proposed approach is efficient, robust, and better than the TMFL. Besides, the equivalent stress in this case is lower than the allowable stress of proposed material. It satisfies the design objectives for the BAM. The optimal results are satisfied with initial requirements.

4.2.3 Case Study 2

Based on the results of sensitivity analysis in Table 5 and Fig. 8, the nonsignificant factors are neglected in modeling and optimization problem. The factors with actual contributions are considered as key design variables. The space of design parameters is decreased, accordingly. Similarly, case study 2 also maximizes both objective functions (F_1 (**X**) and maximizes F_2 (**X**)), simultaneously. Two objective functions are transferred into desirability values and then transformed to MPCI value. The optimization problem is briefly expressed as follows:

Find design variable $\mathbf{X} = [L_1, L_2, T, H_2]^{\mathrm{T}}$

$$\text{Maximize} \quad \text{MPCI}(\mathbf{X})_{\text{case study 2}} \tag{30}$$

S.t.

$$F_1(\mathbf{X}) \geq 1.5$$
$$F_2(\mathbf{X}) \geq 1.7 \text{ mm}$$
$$F_3(\mathbf{X}) \leq \sigma_a$$
$$2.7 \text{ mm} \leq L_1 \leq 3.3 \text{ mm}$$
$$11.25 \text{ mm} \leq L_2 \leq 13.75 \text{ mm}$$

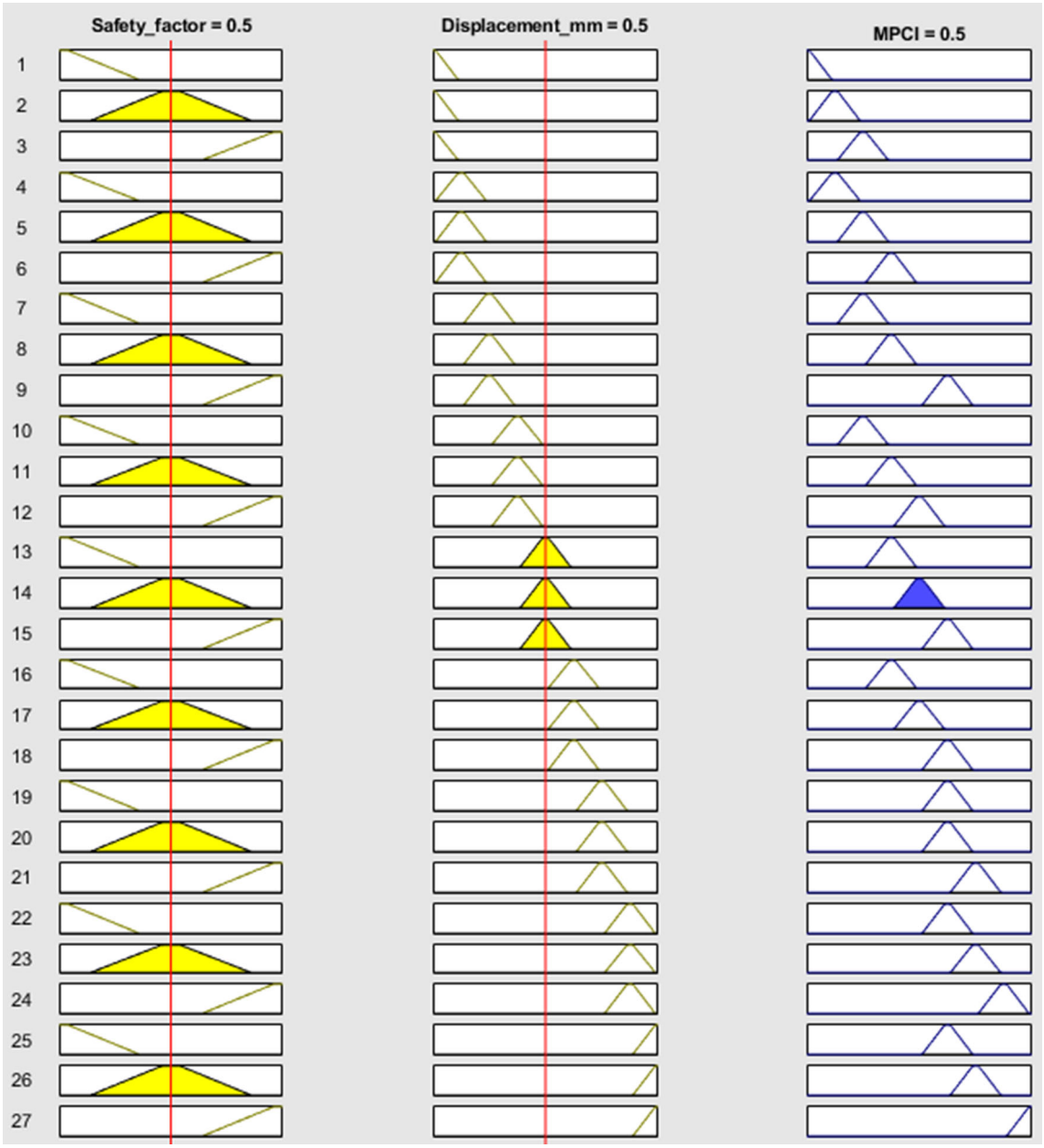

Fig. 13 Twenty-seven fuzzy rules

$$0.45 \text{ mm} \leq T \leq 0.66 \text{ mm}$$
$$1.44 \text{ mm} \leq H_2 \leq 1.76 \text{ mm} \quad (31)$$

The BBD is also used to build eight numerical experiments. The results of displacement, safety factor, and stress are collected by simulations. And then, desirability of displacement and desirability of safety factor are calculated, as given in Table 13. The resulting stress values are under the allowable stress of Al T73-7075.

Next, the MFs for desirability of safety factor are also divided into three levels and the desirability of displacement into seven levels, while the MFs of fuzzy MPCI output are separated into seven levels, as given in Table 9. Subsequently, matrix of fuzzy rules is given in Table 14.

The results of MPCI output are calculated corresponding to the desirability two responses, as given in Table 15.

By taking the values of design variables in Table 13 and the MPCI value of Table 15, ANFIS model is formed for modeling the MPCI. The ANFIS parameters for case study 2 are developed, as given in Table 16.

By using the TMFL, the optimal results are determined at $L_1 = 3.3$ mm, $L_2 = 13.75$ mm, and $T = 0.45$ mm, and $H_2 = 1.44$ mm, as given in Table 17. Based on the TMFL, the optimal displacement and the optimal safety factor are

Table 10 Results of fuzzy MPCI for case study 1

No.	Desirability for F_1 (**X**)	Desirability for F_2 (**X**)	MPCI value
1	0.380999704	0.459061168	0.461
2	0.761457884	0.310888149	0.513
3	0.785413035	0.818092581	0.774
4	0.172242603	0.109036186	0.144
5	0.162202839	0.574090949	0.389
6	0.185263001	0.473312026	0.375
7	0.191556403	0.997841414	0.655
8	0.578640577	0.002158586	0.125
9	0.586262563	0.449888393	0.451
10	0.531301625	0.868582001	0.75
11	0	0.581500805	0.375
12	1	0.294874372	0.581
13	0.319130754	0.136101974	0.226

Table 11 ANFIS parameters for case study 1

Number of nodes	58
Number of linear parameters	72
Number of nonlinear parameters	24
Total number of parameters	96
Number of training data pairs	13
Number of testing data pairs	0
Number of fuzzy rules	18

found at 1.7822 mm and 1.7444, respectively. Subsequently, LAPO algorithm is used to search a global optimum value. The results of proposed hybrid approach determined that the optimal design parameters are L_1= 3.2 mm, L_2= 13.75 mm, and T= 0.45 mm, and H_2 = 1.44 mm. Using the proposed methodology, the optimal displacement and the safety factor are found at 1.8534 mm and 1.7517, respectively. Finally, the predicted MPCI from the proposed approach is greater than that predicted from the TMFL. It means that the estimated solution from the proposed methodology is robust and better than that from the TMFL. Moreover, it finds that the equivalent stress is under the allowable stress of polypropylene. It also satisfies the MOO optimization problem for the bridge mechanism. The optimal results are satisfied with design constraints.

4.2.4 Case Study 3

Based on the results of sensitivity analysis in Table 6 and Fig. 9, the space of design variables is relatively shorted. Case study 3 also simultaneously maximizes F_1 (**X**) and maximizes F_2 (**X**). The computational principle is similar to previous cases. The statement of optimization is stated as follows:

Find design variable $\mathbf{X} = [T, H_1, H_2, L_2]^{\mathrm{T}}$

$$\text{Maximize} \quad \text{MPCI}(\mathbf{X})_{\text{case study 3}} \tag{32}$$

S.t.

$$\begin{aligned} F_1(\mathbf{X}) &\geq 1.5 \\ F_2(\mathbf{X}) &\geq 1.7 \text{ mm} \\ F_3(\mathbf{X}) &\leq \sigma_a \\ 0.45 \text{ mm} \leq T &\leq 0.66 \text{ mm} \\ 4.5 \text{ mm} \leq H_1 &\leq 6.6 \text{ mm} \\ 1.44 \text{ mm} \leq H_2 &\leq 1.76 \text{ mm} \\ 11.25 \text{ mm} \leq L_2 &\leq 13.75 \text{ mm} \end{aligned} \tag{33}$$

Similarly, the BBD is used to build 25 numerical experiments. The results of displacement, safety factor, and stress are collected. And then, desirability values of two responses are calculated, as given in Table 18. The results showed all stress values are smaller than the allowable stress of proposed material.

The MFs for desirability of safety factor include three levels and the ones of displacement are consisted of seven levels, while the MFs of fuzzy MPCI output are divided into seven levels. Subsequently, a matrix of fuzzy rules is given in Table 19.

Table 12 Comparison of different methods for case study 1

Method	Optimal parameters (mm)	Optimal results			
		Safety factor	Displacement (mm)	Stress (MPa)	MPCI
Hybrid of Taguchi method and fuzzy logic	L_2 = 13.75 T= 0.45 H_2= 1.44	F_1 (**X**) = 1.59843	F_2 (**X**) = 1.74598	F_3 (**X**) = 316.2440	0.8600
Proposed hybrid approach	L_2 = 13.80 T= 0.50 H_2= 1.44	F_1 (**X**) = 1.51110	F_2 (**X**) = 1.76860	F_3 (**X**) = 329.9409	0.9458

Table 13 Desirability results of the case study 2

No.	Design variables (unit: mm)				Safety factor	Displacement	Stress	Desirability of safety factor	Desirability of displacement
	L_1	L_2	T	H_2	F_1 (**X**)	F_2 (**X**)-mm	F_3 (**X**)-MPa	d_1	d_2
1	3	12.5	0.555	1.6	1.475086	1.425435	340.9972	0.380999704	0.459061168
2	2.7	11.25	0.555	1.6	1.355915	1.281085	370.9673	0.208136052	0.151590868
3	2.7	13.75	0.555	1.6	1.365908	1.507757	368.2531	0.221368807	0.635027905
4	3.3	11.25	0.555	1.6	1.594497	1.343716	315.4599	0.556001286	0.285199542
5	3.3	13.75	0.555	1.6	1.595557	1.57322	315.2505	0.557064098	0.77468262
6	3	12.5	0.45	1.44	1.583884	1.618079	317.5738	0.535487868	0.868760863
7	3	12.5	0.66	1.44	1.195386	1.480652	420.7844	0.001973228	0.583683153
8	3	12.5	0.45	1.76	1.929505	1.35067	260.6886	0.999456105	0.29350712
9	3	12.5	0.66	1.76	1.431208	1.273322	351.4514	0.316373845	0.136738209
10	3	11.25	0.555	1.44	1.333424	1.43232	377.2244	0.191536892	0.474177478
11	3	13.75	0.555	1.44	1.335427	1.678723	376.6585	0.198020384	0.999037326
12	3	11.25	0.555	1.76	1.620762	1.210485	310.3479	0.580057028	0.001477925
13	3	13.75	0.555	1.76	1.623741	1.420928	309.7785	0.587869103	0.449538192
14	2.7	12.5	0.45	1.6	1.593029	1.440769	315.7506	0.555109724	0.493728964
15	3.3	12.5	0.45	1.6	1.916378	1.504103	262.4743	0.972377667	0.629674025
16	2.7	12.5	0.66	1.6	1.198821	1.338879	419.5791	0.022298955	0.272119021
17	3.3	12.5	0.66	1.6	1.411335	1.402856	356.4001	0.288591536	0.409437348
18	3	11.25	0.45	1.6	1.753896	1.354951	286.7901	0.757750812	0.309056002
19	3	13.75	0.45	1.6	1.774099	1.591645	283.5242	0.781896054	0.816590894
20	3	11.25	0.66	1.6	1.319707	1.263442	381.1451	0.16644982	0.109207526
21	3	13.75	0.66	1.6	1.314954	1.480399	382.523	0.156600146	0.574592749
22	2.7	12.5	0.555	1.44	1.222579	1.520409	411.4253	0.027370717	0.659949831
23		12.5	0.555	1.44	1.459215	1.591396	344.7059	0.350027084	0.811021067
24		12.5	0.555	1.76	1.487116	1.286406	338.2386	0.397431249	0.163290029
25		12.5	0.555	1.76	1.75183	1.343871	287.1283	0.758335407	0.285482182

The value of MPCI is determined according to each value of desirability for objective functions, as given in Table 20.

Subsequently, using the values of design variables in Table 18 and the MPCI value of Table 20, ANFIS model is formed for mapping the design variables and the MPCI. The ANFIS parameters for case study 2 are given in Table 21.

Through the TMFL, the optimal results are determined at T= 0.45 mm, H_1 = 6.5 mm, H_2= 1.44 mm, and L_2 = 13.75 mm, as shown in Table 22. Based on the TMFL, the optimal displacement and the safety factor are found at 1.7454 mm and 1.5904, respectively. Such optimal points are local optimum solutions. Subsequently, the results of proposed hybrid approach showed that the optimal design parameters are at T= 0.47 mm, H_1 = 6.6 mm, H_2= 1.44 mm, and L_2 = 13.75 mm. Using this proposed approach, the optimal displacement and the safety factor are found at 1.7610 mm and 1.5133, respectively. At last, the predicted MPCI from the proposed methodology is effective and better than that from the TMFL. In addition, the equivalent stress is also lower than the allowable stress of the polypropylene. All responses are satisfied the optimal design process for the BAM. The optimal results are satisfied with designer's requirements.

5 Results and Discussion

Based on spaces of design parameters are eliminated, three cases of numerical studies are taken as examples to describe application capacity and effectiveness of the proposed methodology. The performances of proposed methodology are compared with the TMFL. Table 23 summarizes all the optimal solutions for this comparison. In each case study, the optimal factors are used to create a 3D model in SolidWorks 2018 software and then imported into ANSYS 2018 software to evaluate the robustness of proposed hybrid approach by calculating the relative error. This error is calculated as follows:

Table 14 Fuzzy rules matrix for case study 2

No.	Desirability for F_1 (**X**)	Desirability for F_2 (**X**)	MPCI
1	S	T	T
2	M	T	VS
3	L	T	S
4	S	VS	VS
5	M	VS	S
6	L	VS	SM
7	S	S	S
8	M	S	SM
9	L	S	ML
10	S	SM	S
11	M	SM	SM
12	L	SM	M
13	S	M	SM
14	M	M	M
15	L	M	ML
16	S	ML	SM
17	M	ML	M
18	L	ML	ML
19	S	L	ML
20	M	L	ML
21	L	L	L
22	S	VL	ML
23	M	VL	L
24	L	VL	VL
25	S	H	ML
26	M	H	L
27	L	H	H

$$\varepsilon(\%) = \left(\frac{R_p - R_a}{R_a} - 1\right) \times 100 \tag{34}$$

where $\mathfrak{E}$, R_p, and R_a represent the relative error, predicted result from proposed method, and actual result, respectively.

Case study 1: Using the TMFL, the results showed the optimal displacement and safety factor are 1.745 mm and 1.598, respectively. Meanwhile, the proposed hybrid approach predicts the displacement and safety factor about 1.768 mm and 1.511, respectively. By using the proposed method, the relative errors between predicted values and FEA values are very small (around 4%), while the error value is around 1% via using TMFL. Both the proposed methods are reliable tools in this case. According to the Taguchi method, a larger-the-better value of MPCI is a desired value for MOO problem. On the other hand, the proposed hybrid approach has a better performance than the TMFL.

Case study 2: Through the TMFL, the results showed the optimal displacement and safety factor are 1.782 mm and 1.744, respectively. By using the proposed hybrid integration, the optimal displacement and safety factor are found at 1.853 mm and 1.751, respectively. By using the proposed hybrid approach, the relative errors between predicted values and simulated values are around 4.6%, while the error between the predicted value by the TMFL and FEA value is less than 1%. In addition, the MPCI predicted by the proposed hybrid approach is greater than that from TMFL. On the other hand, the performance and prediction accuracy of proposed methodology outperform the TMFL.

Table 15 Results of fuzzy MPCI for case study 2

No.	Desirability for F_1 (**X**)	Desirability for F_2 (**X**)	MPCI
1	0.380999704	0.459061168	0.461
2	0.208136052	0.151590868	0.199
3	0.221368807	0.635027905	0.422
4	0.556001286	0.285199542	0.375
5	0.557064098	0.77468262	0.644
6	0.535487868	0.868760863	0.75
7	0.001973228	0.583683153	0.375
8	0.999456105	0.29350712	0.583
9	0.316373845	0.136738209	0.224
10	0.191536892	0.474177478	0.379
11	0.198020384	0.999037326	0.659
12	0.580057028	0.001477925	0.125
13	0.587869103	0.449538192	0.45
14	0.555109724	0.493728964	0.5
15	0.972377667	0.629674025	0.625
16	0.022298955	0.272119021	0.25
17	0.288591536	0.409437348	0.374
18	0.757750812	0.309056002	0.506
19	0.781896054	0.816590894	0.771
20	0.16644982	0.109207526	0.14
21	0.156600146	0.574592749	0.385
22	0.027370717	0.659949831	0.446
23	0.350027084	0.811021067	0.686
24	0.397431249	0.163290029	0.286
25	0.758335407	0.285482182	0.507

Table 16 ANFIS parameters for case study 2

Number of nodes	55
Number of linear parameters	80
Number of nonlinear parameters	24
Total number of parameters	104
Number of training data pairs	25
Number of testing data pairs	0
Number of fuzzy rules	16

Case study 3: The results showed the optimal displacement and safety factor are 1.745 mm and 1.590, respectively, by using TMFL. Meanwhile, the proposed hybrid approach

Table 17 Comparison of differential methods for case study 2

Method	Optimal parameters (mm)	Optimal results			
		Safety factor	Displacement (mm)	Stress (MPa)	MPCI
Hybrid of Taguchi method and Fuzzy logic	L_1= 3.3 L_2= 13.75 T = 0.45 H_2 = 1.44	$F_1(\mathbf{X}) = 1.7444$	$F_2(\mathbf{X}) = 1.7822$	$F_3(\mathbf{X}) = 289.017$	0.6447
Proposed hybrid approach	L_1= 3.2 L_2= 13.75 T = 0.45 H_2 = 1.44	$F_1(\mathbf{X}) = 1.7517$	$F_2(\mathbf{X}) = 1.8534$	$F_3(\mathbf{X}) = 287.127$	0.8510

Table 18 Desirability results of the case study 3

No.	Design variables (Unit: mm)				Safety factor	Displacement	Stress	Desirability of safety factor	Desirability of displacement
	T	H_1	H_2	L_2	$F_1(\mathbf{X})$	$F_2(\mathbf{X})$-mm	$F_3(\mathbf{X})$-MPa	d_1	d_2
1	0.555	5.5	1.6	12.5	1.475086	1.425435	340.9972	0.380999704	0.459061168
2	0.45	4.5	1.6	12.5	1.789175	1.470534	281.1352	0.810112854	0.557212568
3	0.66	4.5	1.6	12.5	1.335404	1.362406	376.6649	0.198083485	0.325262982
4	0.45	6.5	1.6	12.5	1.749785	1.473127	287.4638	0.753991796	0.560825817
5	0.66	6.5	1.6	12.5	1.300087	1.373929	386.8972	0.14750929	0.347946921
6	0.555	5.5	1.44	11.25	1.333424	1.43232	377.2244	0.18798522	0.475020102
7	0.555	5.5	1.76	11.25	1.620762	1.210485	310.3479	0.578318684	0.00252121
8	0.555	5.5	1.44	13.75	1.335427	1.678723	376.6585	0.19803483	0.998197693
9	0.555	5.5	1.76	13.75	1.623741	1.420928	309.7785	0.589696877	0.44889922
10	0.45	5.5	1.6	11.25	1.753896	1.354951	286.7901	0.754902024	0.310745122
11	0.66	5.5	1.6	11.25	1.319707	1.263442	381.1451	0.162643545	0.109405715
12	0.45	5.5	1.6	13.75	1.774099	1.591645	283.5242	0.782613384	0.816597757
13	0.66	5.5	1.6	13.75	1.314954	1.480399	382.523	0.156359989	0.573108682
14	0.555	4.5	1.44	12.5	1.376799	1.55096	365.3401	0.230938186	0.725249585
15	0.555	6.5	1.44	12.5	1.330449	1.557256	378.0678	0.181671104	0.738663717
16	0.555	4.5	1.76	12.5	1.662364	1.310603	302.5811	0.626016486	0.214616441
17	0.555	6.5	1.76	12.5	1.610023	1.31665	312.4179	0.568588316	0.227499495
18	0.45	5.5	1.44	12.5	1.583884	1.618079	317.5738	0.537466369	0.869201645
19	0.66	5.5	1.44	12.5	1.195386	1.480652	420.7844	0.002994242	0.582633005
20	0.45	5.5	1.76	12.5	1.929505	1.35067	260.6886	1	0.294148563
21	0.66	5.5	1.76	12.5	1.431208	1.273322	351.4514	0.319208187	0.135888722
22	0.555	4.5	1.6	11.25	1.491192	1.309506	337.3141	0.415518867	0.209348358
23	0.555	6.5	1.6	11.25	1.469213	1.314926	342.3601	0.374175383	0.22288113
24	0.555	4.5	1.6	13.75	1.513384	1.535411	332.3676	0.43823691	0.694510338
25	0.555	6.5	1.6	13.75	1.473781	1.540471	341.299	0.372885142	0.707274752

finds the optimal displacement and safety factor approximately 1.761 mm and 1.513, respectively. Both methods find that the relative errors between predicted values and simulated values are around 1%. Moreover, the MPCI predicted by the proposed hybrid approach is higher than that from TMFL. It can conclude that the performance and precision of the proposed approach outperform the Taguchi-based fuzzy logic.

The results of three numerical examples show that the proposed optimization scheme is better than an integration of Taguchi-based fuzzy logic. Among three numerical examples, case study 3 may be chosen as an optimal solution for

Table 19 Fuzzy rules matrix for case study 3

No.	Desirability for F_1 (**X**)	Desirability for F_2 (**X**)	MPCI
1	S	T	T
2	M	T	VS
3	L	T	S
4	S	VS	VS
5	M	VS	S
6	L	VS	SM
7	S	S	S
8	M	S	SM
9	L	S	ML
10	S	SM	S
11	M	SM	SM
12	L	SM	M
13	S	M	SM
14	M	M	M
15	L	M	ML
16	S	ML	SM
17	M	ML	M
18	L	ML	ML
19	S	L	ML
20	M	L	ML
21	L	L	L
22	S	VL	ML
23	M	VL	L
24	L	VL	VL
25	S	H	ML
26	M	H	L
27	L	H	H

Table 20 Results of fuzzy output for case study 3

No.	Desirability for F_1 (**X**)	Desirability for F_2 (**X**)	MPCI
1	0.380999704	0.459061168	0.461
2	0.810112854	0.557212568	0.596
3	0.198083485	0.325262982	0.284
4	0.753991796	0.560825817	0.565
5	0.14750929	0.347946921	0.255
6	0.18798522	0.475020102	0.379
7	0.578318684	0.00252121	0.125
8	0.19803483	0.998197693	0.659
9	0.589696877	0.44889922	0.449
10	0.754902024	0.310745122	0.504
11	0.162643545	0.109405715	0.138
12	0.782613384	0.816597757	0.772
13	0.156359989	0.573108682	0.385
14	0.230938186	0.725249585	0.558
15	0.181671104	0.738663717	0.625
16	0.626016486	0.214616441	0.341
17	0.568588316	0.227499495	0.359
18	0.537466369	0.869201645	0.75
19	0.002994242	0.582633005	0.375
20	1	0.294148563	0.582
21	0.319208187	0.135888722	0.226
22	0.415518867	0.209348358	0.336
23	0.374175383	0.22288113	0.351
24	0.43823691	0.694510338	0.57
25	0.372885142	0.707274752	0.584

Table 21 ANFIS parameters for case study 3

Number of nodes	55
Number of linear parameters	80
Number of nonlinear parameters	24
Total number of parameters	104
Number of training data pairs	25
Number of testing data pairs	0
Number of fuzzy rules	16

MOO design of the bridge mechanism. The reasons are as follows: The displacement and safety factor are found larger than two remain cases. Besides, the equivalent stress IS also under the yield strength of polypropylene. All criteria satisfied the design requirements. The optimal design variables are at $T=$ 0.47 mm, $H_1 =$ 6.6 mm, $H_2=$ 1.44 mm, and $L_2 =$ 13.75. Other remain parameters are constant values. The achieved results demonstrate that the proposed hybrid approach is a robust optimization tool and effectiveness for solving the MOO design for the BAM. The results of this article can be extended for complex optimization fields and other compliant mechanisms.

6 Comparison with Other Metaheuristic Optimization Algorithms

As discussed above, the proposed methodology is outperformed the TMFL for solving MOO design for the BAM. In this section, the proposed algorithm is compared with recent less-parameter optimization algorithms such as Jaya and TLBO. Case 3 is chosen as the final optimal candidate for the BAM. Therefore, ANFIS structure of case 3 is also coupled with Jaya and TLBO algorithms in comparison with the performances. The results indicated that the optimal displacement, safety factor, and MPCI are predicted by the proposed algorithm which are greater than those estimated by the Jaya and TLBO algorithms, as given in Table 24. On the other hand, the proposed methodology has a prediction accuracy better than other methods.

Furthermore, this section implements a statistical investigation in order to evaluate and valid the effectiveness of

Table 22 Comparison of differential methods for case study 3

Method	Optimal parameters (mm)	Optimal results			
		Safety factor	Displacement (mm)	Stress (MPa)	MPCI
Hybrid of Taguchi method and Fuzzy logic	$T = 0.45$ $H_1 = 6.5$ $H_2 = 1.44$ $L_2 = 13.75$	$F_1(\mathbf{X}) = 1.5904$	$F_2(\mathbf{X}) = 1.7454$	$F_3(\mathbf{X}) = 318.163$	0.8538
Proposed hybrid approach	$T = 0.47$ $H_1 = 6.6$ $H_2 = 1.44$ $L_2 = 13.75$	$F_1(\mathbf{X}) = 1.5133$	$F_2(\mathbf{X}) = 1.7610$	$F_3(\mathbf{X}) = 341.234$	0.9959

Table 23 Comparison of the optimal results for three cases

Case study	Method	Optimal factors (mm)	Optimal responses			
			Safety factor	Displacement (mm)	Stress (MPa)	MPCI
Case 1	Hybrid of Taguchi method and fuzzy logic	$L_2 = 13.75$ $T = 0.45$ $H_2 = 1.44$	Predicted $F_1(\mathbf{X}) = 1.598$ FEA $F_1(\mathbf{X}) = 1.582$ $\mathfrak{E} = 1.03\%$	Predicted $F_2(\mathbf{X}) = 1.745$ FEA $F_2(\mathbf{X}) = 1.746$ $\mathfrak{E} = 0.03\%$	Predicted $F_3(\mathbf{X}) = 316.244$ FEA $F_3(\mathbf{X}) = 317.940$ $\mathfrak{E} = 0.53\%$	0.860
	Proposed hybrid approach	$L_2 = 13.80$ $T = 0.50$ $H_2 = 1.44$	Predicted $F_1(\mathbf{X}) = 1.511$ FEA $F_1(\mathbf{X}) = 1.451$ $\mathfrak{E} = 4.12\%$	Predicted $F_2(\mathbf{X}) = 1.768$ FEA $F_2(\mathbf{X}) = 1.721$ $\mathfrak{E} = 2.75\%$	Predicted $F_3(\mathbf{X}) = 329.940$ FEA $F_3(\mathbf{X}) = 346.590$ $\mathfrak{E} = 4.8\%$	0.9458
Case 2	Hybrid of Taguchi method and Fuzzy logic	$L_1 = 3.3$ $L_2 = 13.75$ $T = 0.45$ $H_2 = 1.44$	Predicted $F_1(\mathbf{X}) = 1.744$ FEA $F_1(\mathbf{X}) = 1.734$ $\mathfrak{E} = 0.58\%$	Predicted $F_2(\mathbf{X}) = 1.782$ FEA $F_2(\mathbf{X}) = 1.782$ $\mathfrak{E} = 0.033\%$	Predicted $F_3(\mathbf{X}) = 289.017$ FEA $F_3(\mathbf{X}) = 290.030$ $\mathfrak{E} = 0.35\%$	0.6447
	Proposed hybrid approach	$L_1 = 3.2$ $L_2 = 13.75$ $T = 0.45$ $H_2 = 1.44$	Predicted $F_1(\mathbf{X}) = 1.751$ FEA $F_1(\mathbf{X}) = 1.685$ $\mathfrak{E} = 3.95\%$	Predicted $F_2(\mathbf{X}) = 1.853$ FEA $F_2(\mathbf{X}) = 1.770$ $\mathfrak{E} = 4.68\%$	Predicted $F_3(\mathbf{X}) = 287.127$ FEA $F_3(\mathbf{X}) = 298.500$ $\mathfrak{E} = 3.81\%$	0.8510
Case 3	Hybrid of Taguchi method and fuzzy logic	$T = 0.45$ $H_1 = 6.5$ $H_2 = 1.44$ $L_2 = 13.75$	Predicted $F_1(\mathbf{X}) = 1.590$ FEA $F_1(\mathbf{X}) = 1.596$ $\mathfrak{E} = 0.35\%$	Predicted $F_2(\mathbf{X}) = 1.745$ FEA $F_2(\mathbf{X}) = 1.749$ $\mathfrak{E} = 0.21\%$	Predicted $F_3(\mathbf{X}) = 318.163$ FEA $F_3(\mathbf{X}) = 315.130$ $\mathfrak{E} = 0.96\%$	0.8538
	Proposed hybrid approach	$T = 0.47$ $H_1 = 6.6$ $H_2 = 1.44$ $L_2 = 13.75$	Predicted $F_1(\mathbf{X}) = 1.513$ FEA $F_1(\mathbf{X}) = 1.528$ $\mathfrak{E} = 1.00\%$	Predicted $F_2(\mathbf{X}) = 1.761$ FEA $F_2(\mathbf{X}) = 1.736$ $\mathfrak{E} = 1.41\%$	Predicted $F_3(\mathbf{X}) = 341.234$ FEA $F_3(\mathbf{X}) = 329.040$ $\mathfrak{E} = 0.00\%$	0.9959

Table 24 Comparison between other algorithms with the proposed hybrid approach

Approaches	Displacement (mm)	Safety factor	MPCI
TMFL (T= 0.45 mm, H_1 = 6.5 mm, H_2= 1.44 mm, L_2 = 13.75 mm)	1.745	1.590	0.8538
ANFIS-Jaya (T= 0.45 mm, H_1 = 6.59 mm, H_2= 1.44 mm, L_2 = 13.74 mm)	1.751	1.5243	0.9041
ANFIS-TLBO (T= 0.45 mm, H_1 = 6.6 mm, H_2= 1.44 mm, L_2 = 13.75 mm)	1.748	1.515	0.9041
Proposed algorithm (T= 0.47 mm, H_1 = 6.6 mm, H_2= 1.44 mm, L_2 = 13.75 mm)	1.761	1.640	0.9959

Table 25 Wilcoxon signed rank test for the displacement

Number of tests	Proposed algorithm versus ANFIS-Jaya		
	Wilcoxon statistic	p value	Estimated median difference
45	0.0	0.000	− 0.01
Number of tests	Proposed algorithm versus ANFIS-TLBO		
	Wilcoxon statistic	p value	Estimated median difference
45	0.0	0.000	− 0.013

Table 26 Wilcoxon signed rank test for the safety factor

Number of tests	Proposed algorithm versus ANFIS-Jaya		
	Wilcoxon statistic	p value	Estimated median difference
45	0.0	0.000	− 0.1157
Number of tests	Proposed algorithm versus ANFIS-TLBO		
	Wilcoxon statistic	p value	Estimated median difference
45	0.0	0.000	− 0.125

the proposed hybrid algorithm in comparison with the Jaya algorithm and TLBO algorithm. In this study, two criteria are employed, including the Wilcoxon's signed rank test and Friedman test [63–65]. The computational simulations are conducted with 45 runs for each algorithm. The Wilcoxon's signed rank test is performed for safety factor and displacement at 5% significant level and 95% confidence intervals. As given in Tables 25 and 26, a null hypothesis is assumed that there is no significant difference between mean values of the two algorithms. This statistical analysis is implemented in Minitab 18 software. The results revealed that p value is less than 0.05 (5% significance level). On the other hand, it is a useful evidence against the null hypothesis. As a result, there is a statistical difference between the proposed algorithm and Jaya and TLBO algorithms. Also, it confirms that the proposed hybrid algorithm has a performance effectiveness greater than other algorithms.

Subsequently, Friedman test is analyzed, and the results showed that the p value is less than 0.05. It means that the null hypothesis is rejected. It also confirms that there is a difference between the proposed hybrid optimization approach and the two other algorithms, as given in Tables 27 and 28. Moreover, the effectiveness of the proposed hybrid algorithm is better than ANFIS-based Jaya algorithm and ANFIS-based TLBO algorithm. Besides, the median responses for the proposed algorithm are greater than those of two other algorithms. So, the proposed approach is more effective tool than the other algorithms.

Table 27 Friedman test for displacement

Algorithm	Number of tests	Median	Sum of ranks
ANFIS-Jaya	45	1.75100	90
ANFIS-TLBO	45	1.74800	45
Proposed algorithm	45	1.76100	135
Overall	135	1.75333	
DF	Chi Square	p value	
2	90	0.000	
Null hypothesis	H0: All treatment effects are zero		
Alternative hypothesis	H1: Not all treatment effects are zero		

Table 28 Friedman test for safety factor

Algorithm	Number of tests	Median	Sum of ranks
ANFIS-Jaya	45	1.52430	90
ANFIS-TLBO	45	1.51500	45
Proposed algorithm	45	1.64000	135
Overall	135	1.55977	
DF	Chi-square	*p* value	
2	90	0.000	
Null hypothesis	H0: All treatment effects are zero		
Alternative hypothesis	H1: Not all treatment effects are zero		

7 Conclusions

This paper developed a new hybrid optimization methodology to solve a MOO design for compliant mechanism. The BAM with three numerical cases is studied to confirm the performance efficiency of the proposed hybrid approach. The hybrid optimizing method is a combination of statistical technique, FEM, desirability function approach, fuzzy logic system, ANFIS, and LAPO algorithm. It is considered as a statistical-based intelligent computation. The proposed approach is recommended to search a global solution to overcome limitation of the TMFL.

A 3D FEM model is created, and BBD is used to build experimental matrix. Numerical data are then collected through FEM simulations. Based on the numerical results, a sensitivity investigation is analyzed by using ANOVA and Taguchi method. The refinement process for design variables is carried out to redetermine the searching spaces of design parameters. Next, the desirability values of the safety factor and the displacement are computed, and the results are put into the FIS. The ANFIS technique is then developed to map the refined design variables and the MPCI. The LAPO algorithm is extended to maximize the MPCI.

The results showed that the predicting accuracy of proposed hybrid methodology is better than that of the conventional TMFL. Case study 3 is considered as the optimal candidate of the BAM since it satisfies all design's demands. Finally, Wilcoxon signed rank test and Friedman test are analyzed to compare the performances of the proposed approach with the ANFIS-based Jaya algorithm and ANFIS-based TLBO algorithm. The results showed the performance efficiency of proposed approach is better than those of other approaches. The proposed methodology is expected to be an efficient technique for related complex optimization problems and related compliant mechanisms.

Future work will focus on the time and space of the proposed hybrid approach. Besides, a few physical prototypes are fabricated and extra experimentations are conducted to verify the predicted simulation results and the proposed hybrid method.

Acknowledgements This research is funded by Vietnam National Foundation for Science and Technology Development (NAFOSTED) under Grant No. 107.01-2019.14.

Compliance with Ethical Standards

Conflict of interest The authors declare that they have no conflict of interest.

References

1. Hopkins, J.B.; Culpepper, M.L.: Synthesis of precision serial flexure systems using freedom and constraint topologies (FACT). Precis. Eng. (2011). https://doi.org/10.1016/j.precisioneng.2011.04.006
2. Choi, K.; Lee, J.J.; Kim, G.H.; Lim, H.J.; Kwon, S.G.: Amplification ratio analysis of a bridge-type mechanical amplification mechanism based on a fully compliant model. Mech. Mach. Theory **121**, 355–372 (2018). https://doi.org/10.1016/j.mechmachtheory.2017.11.002
3. Zhou, X.; Xu, H.; Cheng, J.; Zhao, N.; Chen, S.C.: Flexure-based Roll-to-roll Platform: a practical solution for realizing large-area microcontact printing. Sci. Rep. **5**, 1–10 (2015). https://doi.org/10.1038/srep10402
4. Kim, G.W.; Kim, J.: Compliant bistable mechanism for low frequency vibration energy harvester inspired by auditory hair bundle structures. Smart Mater. Struct. (2013). https://doi.org/10.1088/0964-1726/22/1/014005
5. Sun, X.; Yang, B.: A new methodology for developing flexure-hinged displacement amplifiers with micro-vibration suppression for a giant magnetostrictive micro drive system. Sens. Actuators A: Phys. (2017). https://doi.org/10.1016/j.sna.2017.04.009
6. Liu, M.; Zhang, X.; Fatikow, S.: Design and analysis of a multi-notched flexure hinge for compliant mechanisms. Precis. Eng. **48**, 292–304 (2017). https://doi.org/10.1016/j.precisioneng.2016.12.012
7. Howell, L.L.; Magleby, S.P.; Olsen, B.M.: Handbook of Compliant Mechanisms. Wiley, Hoboken (2013)
8. Chen, S.; Ling, M.; Zhang, X.: Design and experiment of a millimeter-range and high-frequency compliant mechanism with two output ports. Mech. Mach. Theory **126**, 201–209 (2018). https://doi.org/10.1016/j.mechmachtheory.2018.04.003
9. Teo, T.J.; Chen, I.M.; Yang, G.; Lin, W.: A generic approximation model for analyzing large nonlinear deflection of beam-based flexure joints. Precis. Eng. **34**, 607–618 (2010). https://doi.org/10.1016/j.precisioneng.2010.03.003
10. Parvari Rad, F.; Vertechy, R.; Berselli, G.; Parenti-Castelli, V.: Analytical compliance analysis and finite element verification of spherical flexure hinges for spatial compliant mechanisms. Mech. Mach. Theory **101**, 168–180 (2016). https://doi.org/10.1016/j.mechmachtheory.2016.01.010
11. Wu, J.; Zhang, Y.; Cai, S.; Cui, J.: Modeling and analysis of conical-shaped notch flexure hinges based on NURBS. Mech. Mach. Theory (2018). https://doi.org/10.1016/j.mechmachtheory.2018.07.005
12. Midha, A.; Howell, L.L.; Norton, T.W.: Limit positions of compliant mechanisms using the pseudo-rigid-body model concept. Mech. Mach. Theory **35**, 99–115 (2000). https://doi.org/10.1016/S0094-114X(98)00093-7

13. Howell, L.L.: Compliant Mechanisms. Wiley, Hoboken (2011)
14. Lobontiu, N.: Compliant Mechanisms: Design of Flexure Hinges. CRC Press, Boca Raton (2002)
15. Koseki, Y.; Tanikawa, T.; Koyachi, N.; Arai, T.: Kinematic analysis of a translational 3-d.o.f. micro-parallel mechanism using the matrix method. Adv. Robot. **16**, 251–264 (2002). https://doi.org/10.1163/156855302760121927
16. Ling, M.; Cao, J.; Jiang, Z.; Lin, J.: Theoretical modeling of attenuated displacement amplification for multistage compliant mechanism and its application. Sens. Actuators A: Phys. **249**, 15–22 (2016). https://doi.org/10.1016/j.sna.2016.08.011
17. Ling, M.; Cao, J.; Pehrson, N.: Kinetostatic and dynamic analyses of planar compliant mechanisms via a two-port dynamic stiffness model. Precis. Eng. **57**, 149–161 (2019). https://doi.org/10.1016/j.precisioneng.2019.04.004
18. Smith, S.T.; Chetwynd, D.G.; Bowen, D.K.: Design and assessment of monolithic high precision translation mechanisms. J. Phys. E (1987). https://doi.org/10.1088/0022-3735/20/8/005
19. Awtar, S.; Sen, S.: A generalized constraint model for two-dimensional beam flexures: nonlinear load-displacement formulation. J. Mech. Des. Trans. ASME **132**, 0810081–08100811 (2010). https://doi.org/10.1115/1.4002005
20. Xu, Q.; Li, Y.: Analytical modeling, optimization and testing of a compound bridge-type compliant displacement amplifier. Mech. Mach. Theory **46**, 183–200 (2011). https://doi.org/10.1016/j.mechmachtheory.2010.09.007
21. Zhu, W.Le; Zhu, Z.; Guo, P.; Ju, B.F.: A novel hybrid actuation mechanism based XY nanopositioning stage with totally decoupled kinematics. Mech. Syst. Signal Process. **99**, 747–759 (2018). https://doi.org/10.1016/j.ymssp.2017.07.010
22. Zhu, B.; Zhang, X.; Wang, N.: Topology optimization of hinge-free compliant mechanisms with multiple outputs using level set method. Struct. Multidiscip. Optim. **47**, 659–672 (2013). https://doi.org/10.1007/s00158-012-0841-1
23. Wang, N.; Zhang, Z.; Zhang, X.; Cui, C.: Optimization of a 2-DOF micro-positioning stage using corrugated flexure units. Mech. Mach. Theory **121**, 683–696 (2018). https://doi.org/10.1016/j.mechmachtheory.2017.11.021
24. Liu, M.; Zhang, X.; Fatikow, S.: Design and analysis of a high-accuracy flexure hinge. Rev. Sci. Instrum. (2016). https://doi.org/10.1063/1.4948924
25. Edwards, K.L.: Compliant mechanisms. Mater. Des. (2002). https://doi.org/10.1016/s0261-3069(01)00088-7
26. Dao, T.P.; Huang, S.C.: Design and multi-objective optimization for a broad self-amplified 2-DOF monolithic mechanism. Sadhana - Acad. Proc. Eng. Sci. **42**, 1527–1542 (2017). https://doi.org/10.1007/s12046-017-0714-9
27. Choi, K.B.; Han, C.S.: Optimal design of a compliant mechanism with circular notch flexure hinges. Proc. Inst. Mech. Eng. Part C J. Mech. Eng. Sci. **221**, 385–392 (2007). https://doi.org/10.1243/09544406JMES312
28. Fossati, G.G.; Miguel, L.F.F.; Casas, W.J.P.: Multi-objective optimization of the suspension system parameters of a full vehicle model. Optim. Eng. **20**, 151–177 (2019). https://doi.org/10.1007/s11081-018-9403-8
29. Dao, T.P.; Ho, N.L.; Nguyen, T.T.; Le, H.G.; Thang, P.T.; Pham, H.T.; Do, H.T.; Tran, M.D.; Nguyen, T.T.: Analysis and optimization of a micro-displacement sensor for compliant microgripper. Microsyst. Technol. **23**, 5375–5395 (2017). https://doi.org/10.1007/s00542-017-3378-9
30. Ling, M.; Cao, J.; Jiang, Z.; Lin, J.: A semi-analytical modeling method for the static and dynamic analysis of complex compliant mechanism. Precis. Eng. **52**, 64–72 (2018). https://doi.org/10.1016/j.precisioneng.2017.11.008
31. Tian, Y.; Shirinzadeh, B.; Zhang, D.: Closed-form compliance equations of filleted V-shaped flexure hinges for compliant mechanism design. Precis. Eng. **34**, 408–418 (2010). https://doi.org/10.1016/j.precisioneng.2009.10.002
32. Costa, N.R.; Lourenço, J.; Pereira, Z.L.: Desirability function approach: a review and performance evaluation in adverse conditions. Chemom. Intell. Lab. Syst. **107**, 234–244 (2011). https://doi.org/10.1016/j.chemolab.2011.04.004
33. Pawade, R.S.; Joshi, S.S.: Multi-objective optimization of surface roughness and cutting forces in high-speed turning of Inconel 718 using Taguchi grey relational analysis (TGRA). Int. J. Adv. Manuf. Technol. (2011). https://doi.org/10.1007/s00170-011-3183-z
34. Dao, T.-P.: Multiresponse optimization of a compliant guiding mechanism using hybrid Taguchi-grey based fuzzy logic approach. Math. Probl. Eng. (2016). https://doi.org/10.1155/2016/5386893
35. Arasu, M.V.; Arokiyaraj, S.; Viayaraghavan, P.; Kumar, T.S.J.; Duraipandiyan, V.; Al-Dhabi, N.A.; Kaviyarasu, K.: One step green synthesis of larvicidal, and azo dye degrading antibacterial nanoparticles by response surface methodology. J. Photochem. Photobiol. B Biol. **190**, 154–162 (2019). https://doi.org/10.1016/j.jphotobiol.2018.11.020
36. Jiang, P.; Wang, C.; Zhou, Q.; Shao, X.; Shu, L.; Li, X.: Optimization of laser welding process parameters of stainless steel 316L using FEM, Kriging and NSGA-II. Adv. Eng. Softw. **99**, 147–160 (2016). https://doi.org/10.1016/j.advengsoft.2016.06.006
37. Wang, B.; Moayedi, H.; Nguyen, H.; Foong, L.K.; Rashid, A.S.A.: Feasibility of a novel predictive technique based on artificial neural network optimized with particle swarm optimization estimating pullout bearing capacity of helical piles. Eng. Comput. (2019). https://doi.org/10.1007/s00366-019-00764-7
38. Koopialipoor, M.; Fahimifar, A.; Ghaleini, E.N.; Momenzadeh, M.; Armaghani, D.J.: Development of a new hybrid ANN for solving a geotechnical problem related to tunnel boring machine performance. Eng. Comput. (2019). https://doi.org/10.1007/s00366-019-00701-8
39. Macura, L.; Voznak, M.: Multi-criteria analysis and prediction of network incidents using monitoring system. J. Adv. Eng. Comput. **1**, 29 (2017). https://doi.org/10.25073/jaec.201711.47
40. Moayedi, H.; Raftari, M.; Sharifi, A.; Jusoh, W.A.W.; Rashid, A.S.A.: Optimization of ANFIS with GA and PSO estimating α ratio in driven piles. Eng. Comput. (2019). https://doi.org/10.1007/s00366-018-00694-w
41. Sreedhara, B.M.; Rao, M.; Mandal, S.: Application of an evolutionary technique (PSO–SVM) and ANFIS in clear-water scour depth prediction around bridge piers. Neural Comput. Appl. **6**, 1–15 (2018). https://doi.org/10.1007/s00521-018-3570-6
42. Le Chau, N.; Dao, T.P.; Dang, V.A.: An efficient hybrid approach of improved adaptive neural fuzzy inference system and teaching learning-based optimization for design optimization of a jet pump-based thermoacoustic-Stirling heat engine. Neural Comput. Appl. (2019). https://doi.org/10.1007/s00521-019-04249-y
43. Keshtiara, M.; Golabi, S.; Tarkesh Esfahani, R.: Multi-objective optimization of stainless steel 304 tube laser forming process using GA. Eng. Comput. (2019). https://doi.org/10.1007/s00366-019-00814-0
44. Wang, D.; Tan, D.; Liu, L.: Particle swarm optimization algorithm: an overview. Soft Comput. (2018). https://doi.org/10.1007/s00500-016-2474-6
45. Dao, T.-P.; Huang, S.-C.; Le Chau, N.: Robust parameter design for a compliant microgripper based on hybrid Taguchi-differential evolution algorithm. Microsyst. Technol. (2017). https://doi.org/10.1007/s00542-017-3534-2
46. Dao, T.-P.; Huang, S.-C.; Thang, P.T.: Hybrid Taguchi-cuckoo search algorithm for optimization of a compliant focus positioning platform. Appl. Soft Comput. J. (2017). https://doi.org/10.1016/j.asoc.2017.04.038

47. Senkerik, R.; Zelinka, I.; Pluhacek, M.: Chaos-based optimization—a review. J. Adv. Eng. Comput. **1**, 68 (2017). https://doi.org/10.25073/jaec.201711.51
48. Zatloukal, F.; Znoj, J.: Malware detection based on multiple PE headers identification and optimization for specific types of files. J. Adv. Eng. Comput. **1**, 153 (2017). https://doi.org/10.25073/jaec.201712.64
49. Chernogorov, I.; Polyakh, V.; Yarakhmedov, O.: Search optimization opportunities of modified self-organizing migrating algorithm in multi-extremal tasks environment. J. Adv. Eng. Comput. **1**, 144 (2017). https://doi.org/10.25073/jaec.201712.60
50. Dinh-Cong, D.; Pham-Duy, S.; Nguyen-Thoi, T.: Damage detection of 2D frame structures using incomplete measurements by optimization procedure and model reduction. J. Adv. Eng. Comput. **2**, 164 (2018). https://doi.org/10.25073/jaec.201823.203
51. Venkata Rao, R.: Review of applications of TLBO algorithm and a tutorial for beginners to solve the unconstrained and constrained optimization problems. Decis. Sci. Lett. **5**, 1–30 (2016). https://doi.org/10.5267/j.dsl.2015.9.003
52. Nenavath, H.; Jatoth, R.K.: Hybrid SCA–TLBO: a novel optimization algorithm for global optimization and visual tracking. Neural Comput. Appl. **6**, 1–30 (2018). https://doi.org/10.1007/s00521-018-3376-6
53. Rao, R.V.; Keesari, H.S.; Oclon, P.; Taler, J.: An adaptive multi-team perturbation-guiding Jaya algorithm for optimization and its applications. Eng. Comput. (2019). https://doi.org/10.1007/s00366-019-00706-3
54. Nematollahi, A.F.; Rahiminejad, A.; Vahidi, B.: A novel physical based meta-heuristic optimization method known as lightning attachment procedure optimization. Appl. Soft Comput. J. **59**, 596–621 (2017). https://doi.org/10.1016/j.asoc.2017.06.033
55. Derringer, G.; Suich, R.: Simultaneous optimization of several response variables. J. Qual. Technol. **12**, 214–219 (1980). https://doi.org/10.1080/00224065.1980.11980968
56. Díaz-Cortés, M.A.; Cuevas, E.; Gálvez, J.; Camarena, O.: A new metaheuristic optimization methodology based on fuzzy logic. Appl. Soft Comput. J. **61**, 549–569 (2017). https://doi.org/10.1016/j.asoc.2017.08.038
57. Zhou, J.; Li, C.; Arslan, C.A.; Hasanipanah, M.; Bakhshandeh Amnieh, H.: Performance evaluation of hybrid FFA-ANFIS and GA-ANFIS models to predict particle size distribution of a muckpile after blasting. Eng. Comput. (2019). https://doi.org/10.1007/s00366-019-00822-0
58. Foroughi Nematollahi, A.; Rahiminejad, A.; Vahidi, B.: A novel multi-objective optimization algorithm based on lightning attachment procedure optimization algorithm. Appl. Soft Comput. J. **75**, 404–427 (2019). https://doi.org/10.1016/j.asoc.2018.11.032
59. Zheng, T.; Luo, W.: An enhanced lightning attachment procedure optimization with quasi-opposition-based learning and dimensional search strategies. Comput. Intell. Neurosci. **2019**, 1–24 (2019). https://doi.org/10.1155/2019/1589303
60. Chen, G.; Gou, Y.; Zhang, A.: Synthesis of compliant multistable mechanisms through use of a single bistable mechanism. J. Mech. Des. Trans. ASME (2011). https://doi.org/10.1115/1.4004543
61. Huang, S.-C.; Dao, T.-P.: Design and computational optimization of a flexure-based XY positioning platform using FEA-based response surface methodology. Int. J. Precis. Eng. Manuf. (2016). https://doi.org/10.1007/s12541-016-0126-5
62. Dao, T.-P.; Huang, S.-C.: Design, fabrication, and predictive model of a 1-dof translational flexible bearing for high precision mechanism. Trans. Can. Soc. Mech. Eng. **39**, 419–429 (2015)
63. García, S.; Fernández, A.; Luengo, J.; Herrera, F.: A study of statistical techniques and performance measures for genetics-based machine learning: accuracy and interpretability. Soft. Comput. (2009). https://doi.org/10.1007/s00500-008-0392-y
64. Li, L.M.; Lu, K.Di; Zeng, G.Q.; Wu, L.; Chen, M.R.: A novel real-coded population-based extremal optimization algorithm with polynomial mutation: a non-parametric statistical study on continuous optimization problems. Neurocomputing (2016). https://doi.org/10.1016/j.neucom.2015.09.075
65. García, S.; Molina, D.; Lozano, M.; Herrera, F.: A study on the use of non-parametric tests for analyzing the evolutionary algorithms' behaviour: a case study on the CEC'2005 special session on real parameter optimization. J. Heuristics **15**, 617–644 (2009). https://doi.org/10.1007/s10732-008-9080-4